

St. John's University

**St. John's Scholar**

---

Theses and Dissertations

---

2019

**INTRANASAL DELIVERY OF INSULIN BY NANOEMULSION  
SYSTEM**

Darshana Mahendrakumar Shah

Follow this and additional works at: [https://scholar.stjohns.edu/theses\\_dissertations](https://scholar.stjohns.edu/theses_dissertations)



Part of the [Pharmacy and Pharmaceutical Sciences Commons](#)

---

**INTRANASAL DELIVERY OF INSULIN BY NANOEMULSION SYSTEM**

A dissertation submitted in partial fulfillment  
of the requirements for the degree of

**DOCTOR OF PHILOSOPHY**

to the faculty of the

**DEPARTMENT OF GRADUATE DIVISION**

of

**COLLEGE OF PHARMACY AND HEALTH SCIENCES**

at

**ST. JOHN'S UNIVERSITY**

New York

by

**DARSHANA SHAH**

Date Submitted: 01/29/2019

Date Approved: 01/29/2019

---

**Darshana Shah**

---

**Jun Shao, Ph.D.**

©: Copyright by Darshana Shah 2019

All Rights Reserved

## ABSTRACT

### INTRANASAL DELIVERY OF INSULIN BY NANOEMULSION SYSTEM

Darshana Shah

The main objective of this research was to develop an o/w nanoemulsion dosage form of insulin for intranasal delivery where insulin is loaded into the oil phase of the nanoemulsion for enhanced absorption. When loaded into the lipid droplets (oil phase), insulin can be protected from enzymatic degradation, can permeate through the mucus gel barrier in a comparatively efficient manner and can be absorbed through transcellular permeation along with paracellular route.

To incorporate lipophilicity to insulin molecule, several complexes of insulin with various amphiphiles were developed to load it into the oil phase. The cytotoxicity of these amphiphiles and the developed nanoemulsions was tested on the human nasal epithelial cells *in vitro*. An optimized formulation with high loading of insulin and low *in vitro* cytotoxicity was developed and characterized.

To predict the absorption of insulin through nasal membrane *in vivo* by the nanoemulsion system, the insulin-loaded nanoemulsion along with controls was tested for the transport across human nasal epithelial cell monolayer *in vitro*. The nanoemulsion significantly ( $p < 0.01$ ) enhanced the permeation of insulin by three times as compared to the insulin solution.

The *in vivo* absorption of insulin after intranasal delivery of the insulin-loaded nanoemulsion was evaluated in anesthetized rats. The results show that the maximum

plasma concentration ( $C_{\max}$ ) and the bioavailability (relative to the subcutaneous delivery) of the insulin-loaded nanoemulsion was 255.9  $\mu\text{U}/\text{ml}$  and 68 %, respectively, while the intranasal delivery of the insulin solution resulted only 5.8  $\mu\text{U}/\text{ml}$  of  $C_{\max}$  and 5% of relative bioavailability. Intranasal delivery of 3.6 IU/kg insulin in nanoemulsion decreased the plasma glucose level remarkably, achieving a maximum reduction of 70%, and the glucose reduction activity lasted for the whole experimental period of 4 h.

These results demonstrate that the nanoemulsion significantly enhanced insulin absorption through intranasal delivery, indicating that the developed nanoemulsion system offers a promising approach for intranasal delivery of insulin.

**DEDICATED TO**

*The Almighty God, my grandmother, my parents Mahendra  
Shah and Vina Shah, and my siblings for their blessings, love,  
their sacrifices made along this journey and unconditional support.*

## ACKNOWLEDGEMENTS

First and foremost, I would like to thank The Almighty God for providing me with the opportunity to undertake this research, the strength, guidance and ability to carry it forward and complete it satisfactorily.

I would like to express my deepest and sincerest gratitude to my mentor, my guide and an amazing human being Dr. Jun Shao. Personally, and professionally this journey wouldn't have been the same without his support and care. I am so thankful to him for his continuous support, guidance, suggestions, sharing his knowledge, teaching us how to think outside of the box and most importantly for inspiring us to be better human beings and to have faith in God. This work wouldn't have been possible if he wouldn't have believed in me. Thank you for everything Dr. Shao, I am so grateful to have you known as a person and having you as my mentor.

This journey wouldn't have been possible without my family's support. I am utterly grateful to my grandmother Kanchan Shah for always being the source of strength, inspiration and courage for me. I miss you Baa; I know you are watching over me and showering me with your blessings. I am so thankful to my parents Mahendra Shah and Vina Shah for their unconditional love, understanding, care and sacrifices they have made along this journey. They have taught me how to be strong, not lose faith and not give up during difficult times. I am thankful to my siblings Bhavya Shah and Hemal Shah for believing in me and standing by my side through my thick and thins. I would also like to thank my aunt Kanak Shah and Kalpana Shah, my brother-in-law Ronak Shah, my sister-

in-law Krima Shah and my uncle Pankaj Shah for their support, love and care during this journey.

I would like to thank my committee members, Dr. Bhagwan Rohera, Dr. Abu Serajuddin, Dr. Zhe-Sheng Chen, Dr. Sabesan Yoganathan & Dr. Ketankumar Patel for their invaluable support, help, guidance and suggestions. I would also like to thank Dr. Blase Billack for serving as chair for my defense committee and his guidance.

I would like to thank my current and previous lab mates (Prachi J., Jason, Yuxing, Kanyaphat, Atanu, Leo, Mayuri, Pulkit, Marie, Prachi S. and Micheal) for making this journey so much more enjoyable and worth. I am so grateful to them for their help, assistance, for cheering me up in my dull days, endless discussions about science, life and everything else in between. I thank you all from bottom of my heart for everything you guys have done for me. This wouldn't have been possible without your support.

I am so grateful to Dr. Louis Trombetta, Dr Abu Serajuddin, Dr. Blase Billack and Dr. Woon-Kai Low for allowing me to use their lab instruments and resources. I would like to thank Dr. Ashley Thomas Martino for helping me with learning ELISA technique and collaborating with us for histology study. I am so thankful to Igor Ban (Dr. Martino's student) for coming on board with me for histology study and making it possible when it seemed impossible. I would also like to thank other faculty members and fellow graduate students of Pharmacy school for their support and assistance during my stay at SJU.

I would like to thank PHS department and Dean's office for helping, assisting and teaching positions. My sincere thanks to Dr. Marc Gillespie, Dr. Vijaya Korlipara and Sawanee Khongsawatwaja for their continuous support and guidance. I would like to

thank Dr. Carvalho, Pratibha, Susana, Joyce and Velda for guiding me through my teaching journey, their support and teaching me the important aspects of professional job. I would like to thank Luz Mery for her constant support, care and help.

I am so grateful to Dr. Harry Mankodi for his continuous support, guidance and help. He has always been there for me throughout this journey and I am so blessed to have him in my life. I can't thank enough to Dr. Priti Patel and Dr. Sahamat Khan for their selfless help.

I would like to thank Arlene King from Dean's office for being that guardian angel for me and always showing me the brighter side of any tough situation, I can't thank her enough for everything that she has done for me. I have always felt that comfort and love of a family member from her and I will be always grateful to her for being there for me throughout this journey. Thank you, Arlene.

I would like to thank all my close friends, my nieces and nephews, my cousins and my loved ones who have walked this journey with me hand in hand. This one is for you all. Thank you for your support, love, laughter, and most importantly spending quality time with me in person and through video calls. This journey would have been so lonely without you all being part of it considering my late-night lab stays. Thank you for always inspiring me to do better.

I would like to thank Suzette and Jason from science supply for their continued support. I would also like to thank Eileen, Helen, Jessica and Ernie from animal care center for helping and guiding me through my animal study. I am so thankful to every single person who has helped me along this journey.

I would like to thank St. John's University for giving me this opportunity, providing the resources and beautiful campus. Lastly, I would like to thank New York city for making me the person I am today. Thank you, New York.

## TABLE OF CONTENTS

DEDICATIONS.....	ii
ACKNOWLEDGEMENTS.....	iii
LIST OF TABLES.....	xii
LIST OF FIGURES .....	xiii
CHAPTER 1. INTRODUCTION .....	1
1.1. Introduction .....	1
1.2. Nasal Cavity .....	3
1.3. Limitations of Intranasal Delivery .....	5
CHAPTER 2. LITERATURE REVIEW, HYPOTHESIS AND OBJECTIVES .....	8
2.1. Human Insulin .....	9
2.2. Hypothesis.....	15
2.3. Research Objective.....	15
CHAPTER 3. FITC LABELING OF INSULIN AND TRANSPORT OF FITC-INSULIN CONJUGATES THROUGH MDCK CELL MONOLAYER.....	17
3.1. Introduction .....	17
3.2. Materials.....	18
3.3. Methods.....	19
3.3.1. FITC Labeling of Human Insulin .....	19

3.3.2.	HPLC Assay.....	20
3.3.3.	Lipophilicity and Hydrophilicity Assay of the Conjugates .....	22
3.3.4.	Transport of FITC-labeled Insulin through MDCK Cell Monolayer .....	22
3.4.	Results & Discussion .....	23
3.4.1.	FITC Labeling of Human Insulin .....	23
3.4.2.	Lipophilicity and Hydrophilicity of FITC-Insulin.....	28
3.4.3.	Transport of FITC-labeled Insulin through MDCK Cell Monolayer .....	28
3.5.	Conclusion.....	32
CHAPTER 4: FORMULATION DEVELOPMENT AND <i>IN-VITRO</i> STUDY .....		33
4.1.	Introduction .....	33
4.2.	Materials.....	36
4.3.	Methods.....	37
4.3.1.	Development and Characterization of Insulin Loaded Self-emulsified Nanoemulsion Formulations.....	37
4.3.2.	Development of Self-emulsified Nanoemulsion Formulations .....	38
4.3.2.1	Phase Diagram Construction .....	38
4.3.2.2	Droplet size.....	39
4.3.2.3	Dilution test .....	39
4.3.3.	Incorporation of Lipophilicity to Human Insulin Molecule .....	41
4.3.3.1.	Hydrophobic Ion-pairing .....	41

4.3.3.2. Solid Dispersion.....	42
4.3.4. Characterization of Insulin Complexes.....	42
4.3.4.1. Differential Scanning Calorimetry.....	42
4.3.4.2. Partition Coefficient.....	43
4.3.5. Cytotoxic Effect of Nanoemulsion Components and Complexing Agents on Human Nasal Epithelial Cells (HNEpC) .....	43
4.3.6. Preparation of Insulin Loaded Self-emulsified Nanoemulsions .....	44
4.3.6.1. Droplet Size .....	45
4.3.6.2. Leakage of Insulin from the Oil Phase .....	45
4.3.7. Transport of Insulin by Nanoemulsion through Human Nasal Epithelial Cell Monolayer .....	46
4.3.7.1. HNEpC Transport Study .....	46
4.3.7.2. HNEpC Monolayer Integrity Study.....	48
4.3.8. Data Analysis .....	48
4.4. Results .....	49
4.4.1. Formulation Development .....	49
4.4.2. Preparation of Insulin Complexes.....	54
4.4.2.1. Hydrophobic Ion-pairing .....	54
4.4.2.2. Solid Dispersion.....	56
4.4.3. Characterization of Insulin Complexes.....	56

4.4.3.1.	Differential Scanning Calorimetry .....	56
4.4.3.2.	Partition Coefficient .....	59
4.4.4.	Cytotoxicity of Formulation Components and Complexing Agents on Human Nasal Epithelial Cells (HNEpC) .....	61
4.4.5.	Preparation of Insulin Complex Loaded Nanoemulsion.....	66
4.4.5.1.	Droplet size of Ins-SPC Loaded NE-8 Nanoemulsion .....	66
4.4.5.2.	Leakage of Insulin from the Oil Phase to the Aqueous Phase of the Nanoemulsion .....	67
4.4.6.	Transport of Insulin through Human Nasal Epithelial Cell Monolayer .....	72
4.4.7.	Effect of the NE-8 Nanoemulsion on the Integrity of the HNEpC Monolayer .....	76
4.5.	Conclusion.....	80
CHAPTER 5. <i>IN-VIVO</i> ANIMAL STUDY .....		81
5.1.	Introduction .....	81
5.2.	Materials.....	82
5.3.	Methods.....	83
5.3.1.	Animal Study Procedure .....	83
5.3.2.	ELISA Assay .....	84
5.3.3.	Histological Study.....	87
5.4.	Data Analysis .....	87

5.5. Results .....	87
5.5.1. <i>In-vivo</i> Absorption Study .....	87
5.5.2. Histology Study .....	94
5.6. Conclusion.....	96
CHAPTER 6: FUTURE STUDIES .....	97
REFERENCES .....	98

## LIST OF TABLES

Table 1. HPLC gradient elution schedule. ....	21
Table 2. List of materials .....	40
Table 3. Formulation composition, droplet size and polydispersity index (PDI).....	52
Table 4. Effect of dilution with PBS on droplet size of the formulations. ....	53
Table 5. Dispersibility of insulin complexes in the lipid mixture.....	68
Table 6. Droplet size of NE-8 nanoemulsions .....	70
Table 7. Leakage of insulin from various preparations .....	71
Table 8. Droplet size in the donor and receiver side at the end of the transport study through HNEpC monolayer .....	75
Table 9. Animal groups for the <i>in-vivo</i> study .....	86
Table 10. Pharmacokinetic and pharmacodynamic parameters.....	93

## LIST OF FIGURES

Fig. 1. Nasal Cavity .....	4
Fig. 2. Human insulin structure.....	16
Fig. 3 Primary structure of human insulin. ....	25
Fig. 4. Chromatograms of the FITC labeled insulin .....	26
Fig. 5. Chromatograms .....	27
Fig. 6. Permeability coefficient ( $P_{app}$ ), molecular weight and partition coefficient (p) value of unlabeled insulin, mono- and tri-conjugates.....	30
Fig. 7. Transport of mono- and tri-conjugated FITC-Insulin and unlabeled insulin through MDCK monolayer .....	31
Fig. 8. Phase diagram.....	51
Fig. 9. Complexation efficiency (%) vs molar ratio of SDC to insulin .....	55
Fig. 10. Thermograms.....	58
Fig. 11. Partition coefficient .....	60
Fig. 12. Effect of the complexing agents on the viability of HNEpC.....	63
Fig. 13. Effect of surfactant Cremophor RH40 on the viability HNEpC .....	64
Fig. 14. Effect of various nanoemulsions on the viability of HNEpC .....	65
Fig. 15. Pseudo-ternary phase diagram.....	69
Fig. 16. Permeability through HNEpC monolayer .....	74
Fig. 17. Permeability of Propranolol through HNEpC monolayer .....	78
Fig. 18. Permeability of Mannitol through HNEpC monolayer .....	79
Fig. 19. Blood glucose reduction profile .....	91
Fig. 20. Plasma insulin conc. vs time profile.....	92

Fig. 21. Photomicrographs of nasal mucosal membrane ..... 95

# CHAPTER 1. INTRODUCTION

## 1.1. Introduction

Peptide and protein drugs are increasingly becoming a very important class of therapeutic agents. While the peptide and protein therapeutic market has developed significantly in the past decades, delivery challenge has limited the use of these drugs (Bruno et al., 2013). The route of administration has a significant impact on the therapeutic outcome of the drug. The needle and the syringe are a well-established choice of protein and peptide drug delivery. Parenteral route offers the best absorption but has its own disadvantages including lack of patient compliance, safety considerations and high medication cost (Illum, 1991; Muheem et al., 2014). Thus, the noninvasive routes such as oral, pulmonary, transdermal, buccal and nasal routes have been investigated for protein and peptide drug delivery.

Oral route is the most popular for systemic absorption of various systemically acting drugs as it involves ease of administration, large surface area for absorption, patient acceptability and cost savings to the health care industries. However, most of the peptide and protein drugs are poorly absorbed when administered orally due to degradation in gastrointestinal (GI) tract, inefficient transport across the epithelial layer and hepatic first pass metabolism (Muheem et al., 2014).

Therefore, other non-invasive routes have been extensively explored for protein and peptide drug delivery. Owing to the physiological characteristics of the respiratory system, the pulmonary route has received special attention for protein and peptide drug delivery as it offers a large surface area for drug absorption, rapid drug absorption and

avoidance of hepatic first-pass metabolism (Jitendra et al., 2011). Several peptides and proteins have shown enhanced absorption through pulmonary administration. But delivery through this route has some limitations such as insufficient deposition of the drug in deep lungs, local tissue irritation and possibly reduced bioavailability (Klingler et al., 2009).

The buccal mucosa represents an important site for controlled delivery of protein and peptide drug with some advantages such as avoidance of hepatic first-pass metabolism, acidity and protease activity encountered in GI tract (Sudhakar et al., 2006). However, limited studies have been done for protein drug delivery via buccal mucosa as it has relatively low permeability and smaller surface area, and the continuous secretion of saliva leads to subsequent dilution of drug, and swallowing of saliva can potentially lead to the loss of dissolved or suspended drug (Reddy et al., 2011).

Transdermal delivery of protein and peptide drugs offers an appealing alternative to other delivery routes as skin is the most accessible organ of the body with a large surface area and provides a better patient compliance. However, the outermost barrier of skin, stratum corneum which is made up of dead keratinocytes, acts as a significant rate limiting barrier. Also the long term adherence of transdermal patches causes patient discomfort (Kalluri and Banga, 2011).

Recent years have shown that the nasal route can be explored for the systemic delivery of protein and peptide drugs. Intranasal delivery of protein and peptide drugs presents myriad benefits such as ease of administration, noninvasive needle-free administration, rapid onset of action, and the avoidance of gastrointestinal and hepatic first-pass effects (Ko et al., 1998). Nasal mucosa has a high degree of vascularization and

high permeability to small molecules, which enables systemic administration of biopharmaceuticals via this route (Yuba and Kono, 2014).

Conventionally, the nasal route has been used for treatment of local diseases such as nasal allergy, nasal congestion and nasal infection. In recent years the nasal route has been explored for the systemic delivery of drugs such as small molecular and high molecular weight polar drugs, peptides and proteins that are not easily administered via other routes than injection, or where a rapid onset of action is required (Ozsoy et al., 2009).

## **1.2. Nasal Cavity**

The human nasal passage is about 12 cm long and runs from the nostrils to the nasopharynx (Fig. 1) (Gad and Wiley InterScience (Online service), 2008) . The nasal cavity is divided into two halves by the nasal septum and extends posteriorly to the nasopharynx, while the most anterior part of the nasal cavity, the nasal vestibule, opens to the face through the nostril. The atrium is an intermediate region between the vestibule and the respiratory region. The respiratory region, the nasal conchae or turbinates, which occupies the major part of the nasal cavity, possesses lateral walls dividing it into three sections: the superior, middle and inferior nasal turbinates. The presence of these turbinates creates a turbulent airflow through the nasal passages which ensures a better contact between the inhaled air and the mucosal surface (Illum, 2003). Maximum drug absorption in nasal cavity takes place at the respiratory region as it has vast surface area and is rich in vascularity.

The nasal respiratory mucosa is covered with mucus. The mucus is about 5  $\mu\text{m}$  thick and has a viscous gel on the upper part and an aqueous solution layer on the lower part (Arora et al., 2002). Nasal epithelium is covered with new mucus layer approximately every 15 min (Lansley, 1993). The mucosal secretion contains 95% water, 2% mucin, 1% salt, 1% albumin, immunoglobulin, lysozyme, lactoferin and other proteins and 1% lipids. Nasal mucus also contains IgA, IgE and IgG (Lansley, 1993; Ugwoke et al., 2001).

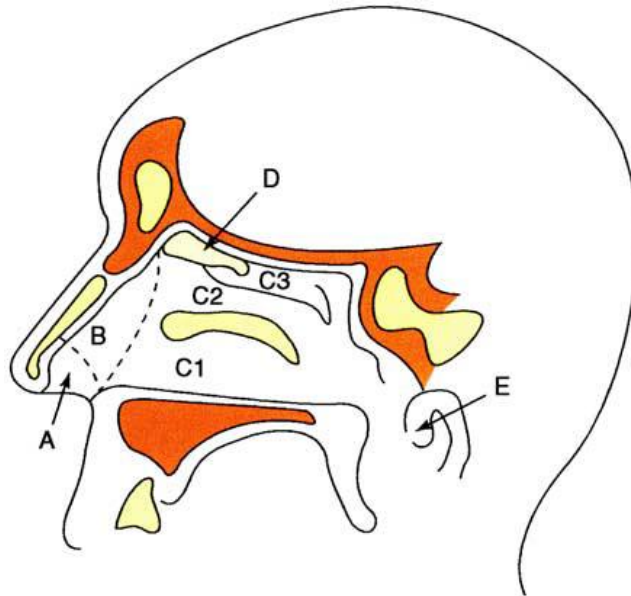


**Fig. 1.** Nasal Cavity: nasal vestibule (A), atrium (B), respiratory area and inferior turbinate (C1), middle turbinate (C2) and superior turbinate (C3), olfactory region (D), and nasopharynx (E) (Gad, 2008).

Compared to other biological membranes the nasal mucosa is relatively porous, and thin, and has a rapid blood flow and a vast absorption area ( $150\text{ cm}^2$ ) with microvilli on the epithelial cells (Ugwoke et al., 2001).

### 1.3. Limitations of Intranasal Delivery

Even though the nasal epithelium is suitable for systemic delivery of a variety of drugs, the drug absorption is limited due to following main factors (Schmidt et al., 1998):

- Limited application volume (25 – 250  $\mu$ l)
- Difficulty in permeability of high molecular weight ( $>1000$  Da) drugs through nasal epithelium
- Mucociliary clearance
- The enzymatic barrier of the epithelium

The volume that can be delivered to the nasal cavity is restricted to 25 – 250  $\mu$ L. Therefore different approaches have been explored to use this volume effectively including the use of solubilizers and gelling agents (Arora et al., 2002). The use of solubilizer increases the aqueous solubility of insoluble compounds and can even promote the nasal absorption of the drug. Gelling agent decreases the drainage and results in increased retention of drug in nasal cavity.

The molecular size of the drug influences intranasal absorption. The rate of permeation is highly sensitive to molecular size for compounds with molecular weight (MW)  $\geq 300$  Daltons (Corbo et al., 1990). A large number of therapeutic agents, peptides and proteins in particular have shown that for compounds  $> 1$  kDa, bioavailability can be directly predicted by MW. In general, the bioavailability of these large molecules ranges from 0.5% to 5% (Donovan and Huang, 1998).

Another factor for low absorption is the rapid clearance of the administered formulation from the nasal cavity due to mucociliary clearance (MCC) mechanism. It is a normal defense mechanism of the nasal cavity that clears mucus as well as substances

adhering to the nasal mucosa (bacteria, allergens etc.) and drains them into the nasopharynx for eventual discharge into the gastrointestinal tract. Whenever a substance is nasally administered, it is cleared from the nasal cavity in about 21 min by MCC (Marttin et al., 1998). Reduced mucociliary clearance increases the contact time of a drug and the mucus membrane and subsequently enhances the drug permeation (Lansley, 1993).

Nasally administered drugs circumvent gastrointestinal and hepatic first-pass effects. However, they might be metabolized to some degree in the lumen of the nasal cavity or during passage across the nasal epithelial barrier because of the presence of metabolic enzymes in nasal tissues. Nasal epithelium and nasal secretions possess a wide range of enzymes. Nasal epithelium contains carboxyl esterases, aldehyde dehydrogenases, epoxide hydrolases, and glutathione S-transferases. They are responsible for the degradation of drugs in nasal mucosa (Yuba and Kono, 2014). The nasal mucosa also includes oxidative phase I and conjugative phase II enzymes. The phase I enzymes include aldehyde dehydrogenase, carboxyl esterase, and carbonic anhydrases; Phase II enzymes include glucuronyl, sulfate and glutathione transferases (Gad and Wiley InterScience (Online service), 2008). Proteolytic enzymes (aminopeptidases and proteases) present in nasal mucosa are believed to be one of the barriers against the absorption of protein & peptide drugs such as calcitonin, insulin and desmopressin (Pires et al., 2009).

Zhou et. al. compared the aminopeptidase activity in nasal, buccal, dermal and intestinal tissue homogenates. The study reported that the nasal homogenates showed half of the intestinal aminopeptidase activity (Zhou and Po, 1990). Although enzymatic

activity is present in the nasal cavity, this activity is generally lower than the enzymatic activity of the gastrointestinal tract, making this route an attractive alternative to the oral delivery of enzymatically labile drugs such as therapeutic peptides and proteins (Hillery et al., 2002).

In spite of these hurdles, the nasal route is still considered to be superior to the oral route for protein and peptide delivery as it avoids harsh GI environment, presents relatively less enzymatic degradation and has highly vascularized epithelial tissue with similar permeability as the small intestine (Arora et al., 2002).

## CHAPTER 2. LITERATURE REVIEW, HYPOTHESIS AND OBJECTIVES

Studies have shown that through nasal delivery, the bioavailability of the peptide and proteins is inversely proportional with their molecular weight and number of amino acids. In other words, the absorption of drugs via nasal mucosa decreases as the molecular weight increases. Absorption is particularly low for high molecular weight drugs applied as simple aqueous solutions. So, several strategies have been employed to improve the nasal bioavailability of proteins and peptides. Most popular approaches can be summarized as follows:

- **Modification of the chemical structure of the drug**

Modification of the chemical structure of the peptides and proteins may increase the metabolic stability and/ or membrane permeability (Nash et al., 2002). The nasal absorption of L-tyrosine and the effect of structural modification on its absorption have been studied by an *in situ* experimental technique (Huang et al., 1985). It was assessed that chemically modified carboxylic acid esters were absorbed 4-10 times faster than L- tyrosine.

- **Enzyme inhibitors**

Proteins and peptide drugs can be applied with enzyme inhibitors to protect them from the enzyme activity present in nasal mucosa (Behl et al., 1998). Inhibitors with a trypsin-inhibiting activity have been proved to be useful in enhancing the nasal absorption of salmon calcitonin (Morimoto et al., 1995).

- **Absorption enhancers**

Inclusion of absorption enhancers (such as bile salts and surfactant, fusidic acid derivatives, phosphatidylcholines and cyclodextrins) may enhance the passage of drugs with polar structure through nasal mucosa (Ozsoy et al., 2000). Calcitonin, a polypeptide of 3.4 kDa, showed enhanced nasal absorption in rats when it was delivered with 5% methylated  $\beta$ -cyclodextrin derivative as an absorption enhancer (Adjei et al., 1992).

- **Novel formulations**

Novel formulations including drug carrier system such as liposomes, gels, lipid emulsions, niosomes, nano and microparticle have been studied to enhance the nasal absorption (Brooking et al., 2001; Gungor et al., 2010; Kumar et al., 2009; Mitra et al., 2000). Nasal administration of insulin-loaded polyacrylic acid microparticles suspended in 1% (w/v) polyacrylic acid gel resulted in a noticeable and sustained hypoglycemic effect for seven hours in normal rabbits (Dondeti, 1991).

## **2.1. Human Insulin**

Insulin is a 51 amino acid peptide that was discovered in 1921 by Frederick Banting and Best, together with MacLeod and Collip (Fig. 2). It is secreted by pancreatic  $\beta$  cells and has the ability to control glucose levels in blood by facilitating glucose uptake into the cells of the organism. The most common therapy for diabetes mellitus is the injection of insulin. But it is a painful and inconvenient approach, resulting in poor patient compliance (Pillai and Panchagnula, 2001). In recent decades, oral delivery of insulin has been widely investigated because it can improve patient compliance (Trehan

and Ali, 1998). However, there are various obstacles for oral administration of insulin, mainly its poor absorption properties, poor absorption from the intestinal lumen and susceptibility to chemical and physiological degradation (Jintapattanakit et al., 2007).

Nasal delivery of insulin may be a suitable approach as it avoids harsh environment of GI and hepatic first pass effect. Multiple studies have been done with different strategies to enhance intranasal absorption of insulin including particulate delivery, inclusion of absorption enhancers, using enzyme inhibitors and lipid-based formulations.

Proteolytic enzyme inhibitors could prevent the hydrolysis of peptide and protein drugs in the nasal cavity and thus, improve the stability of drugs at the absorption site. Aungst and Rogers (Aungst and Rogers, 1988) reported an improvement in intranasal insulin absorption in rats by co-administration of aprotinin, a serine protease inhibitor. Efficacy, relative to an intramuscular dose, was improved from 0.4% for the control insulin solution to 9.6% in the presence of aprotinin. However, proteolytic enzyme inhibitors themselves cannot facilitate the penetration of drugs across the epithelial membrane and therefore, are generally unable to considerably improve bioavailability in the absence of absorption enhancers. Furthermore, the enzyme inhibitors will affect the normal metabolism of the body, resulting in serious side effects. Therefore, enzyme inhibitors do not seem to be an effective and safe method of improving the nasal absorption of insulin.

The use of absorption enhancers or promoters has been the most common approach to improve the nasal absorption of insulin. Ideally, absorption promoters should be rapid-acting, resulting in transient and reversible modulation of the absorptive properties or physiology of the nasal mucosa, and not be absorbed systemically. They should be

devoid of any toxic, irritating or allergic activity. So far, many compounds – such as surfactants (e.g. 0.5% lysophosphatidylcholine (LPC), 0.5% laureth-9, 1.0% sterol glucoside), bile salts and its derivatives (e.g. 1% sodium deoxycholate, 1% sodium taurodihydrofusidate), fatty acids and its derivatives, cyclodextrins, cell penetrating peptides, chelators and cationized polymers – have been investigated as absorption enhancers for nasal delivery of insulin (Aungst and Rogers, 1988; Illum et al., 1989; Moses et al., 1983) . These absorption enhancers are effective in improving the nasal absorption by increasing the nasal fluidity of bilayer membrane and by opening aqueous pores as a result of calcium ion chelation. However, they tend to cause severe nasal irritation and damage nasal membrane at the concentrations required to effectively promote nasal absorption (Davis and Illum, 2003). For example, surfactants such as laureth-9 damages epithelial membrane by dissolving the membrane lipids or proteins, resulting in cell erosion, cell to cell separation and loss of the cilia (J.M. Pezzuto H.R. Manasse, 2013). Haffejee et. al. evaluated the toxicity of LPC on rat nasal epithelium. Transmission electron microscopy (TEM) results showed that 1% w/v LPC caused severe epithelial damage and total loss of ciliated cells (Haffejee et al., 2001). The nasal epithelial layer serves as a defense against infecting organisms, and therefore loss or damage of this layer can cause severe problems.

The mucoadhesive approach has been developed to improve intranasal drug absorption because it could prolong the intimate contact time of the formulation on the nasal mucosa by adhering to the surface of the mucus layer and thereby enhancing the bioavailability. Microspheres have been suggested to exert several mechanisms for absorption-enhancement effects on the nasal delivery of peptides and/or proteins.

Microspheres deposit in the less- or non-ciliated anterior part of the nasal cavity with slower nasal clearance. The bioadhesive effect of the microspheres decreases the rate of clearance of the drug from the nasal cavity and thereby enables a longer contact time with the absorptive epithelium (Edman et al., 1992). The gelled system provides a local high drug concentration in close contact with the epithelial absorptive surface. Furthermore, it has been shown in a study employing monolayers of Caco-2 cells that the absorption of water by the microspheres from the mucus layer can induce reversible and transient shrinking of the epithelial cells and widening of the tight junctions and, therefore, the transport of hydrophilic compounds could be increased (Haffejee et al., 2001). Callens et al. (Callens et al., 2003) demonstrated that the bioavailability of insulin obtained with the powder formulations containing drum-dried waxy maize starch and Carbopol® 974P were significantly higher than those containing maltodextrins and Carbopol® 974P mixtures. The bioavailability of insulin increased as the ratio of Carbopol® 974P increased. The absolute bioavailability in the powder formulation containing drum-dried waxy maize starch and 10% Carbopol® 974P was as high as 14.4%. Morimoto et al. (Matsuyama et al., 2006) reported that the nasal administration of insulin in 0.1% and 1% (w/v) polyacrylic acid gels showed maximum hypoglycemic effects at 30 min and one hour after administration, respectively. However, it is generally difficult to achieve a satisfactory effect for macromolecular drugs by increasing retention time in the nasal cavity alone because it has to simultaneously overcome the physical barrier of the epithelium for a drug to permeate into the systemic circulation.

As nanotechnology-based drug delivery systems have become accessible to fill the pharmaceutical R&D pipeline, nano-sized emulsions (conventionally called

microemulsions) have been one of the most attractive formulations as potential drug carriers to enhance the uptake across nasal mucosal membrane (Sintov et al., 2010). Nanoemulsions are thermodynamically stable systems with the droplet size usually less than 100 nm. Nanoemulsions have been widely studied to increase the bioavailability of poorly water-soluble drugs. Poorly water-soluble drugs are easily dissolved in the oil phase as they are hydrophobic in nature. The mechanisms for the increase in the bioavailability are due to improvement of drug solubilization, protection against enzymatic degradation and the increased surface area of droplets (Rao et al., 2008b). Nanoemulsion formulation has several advantages such as ease of preparation, cost effective and easy to administer to the patient. Literature review indicates that there were only two publications on intranasal delivery of insulin by emulsion formulations.

Mitra et. al. (Mitra et al., 2000) reported that insulin absorption through rat's nasal mucosa was enhanced by o/w emulsion system, where insulin was loaded in the aqueous phase. AUC was observed 4 times higher for o/w insulin loaded emulsion than the insulin buffer solution. The authors had also prepared w/o emulsion where insulin was loaded in the aqueous phase, and did not observe any increase in absorption. Emulsion formulation for this study contained soybean oil, tween 80 and span 80. Measured droplet size for o/w emulsion was around 4  $\mu\text{m}$  whereas w/o showed broader distribution from 1  $\mu\text{m}$  to 10  $\mu\text{m}$ .

Sintov et. al. (Sintov et al., 2010) demonstrated that intranasal delivery of o/w microemulsion system with 20% water content (insulin in the aqueous phase) achieved an absolute bioavailability of 7.5% in rabbit. Bioavailability was observed negligible when the water content was increased to 50% for the o/w microemulsion formulation. The

microemulsion formulation used for this study contained isopropyl palmitate, glyceryl oleate, labrasol and propylene carbonate. Measured droplet size for both w/o & o/w ranged between 10-20 nm by TEM.

In the above two studies, insulin was loaded in the aqueous phase of the emulsion system. First study by Mitra et. al. showed enhanced permeation of insulin by o/w emulsion. This enhancement might be due to the components of the formulation such as surfactants which might have opened the tight junctions of the nasal epithelium. An insulin solution with surfactants probably would show the similar effect, but authors did not study the effect of insulin solution with surfactants. The other possibility for enhanced insulin permeation could be slow mucociliary clearance process due to adherence of the lipid droplets to the nasal epithelial membrane which may be achieved by use of certain mucoadhesive agents.

In the second study by Sintov et al., again, since insulin was in the external aqueous phase, the purpose of forming nanoemulsion was defeated. The enhancement by 20% water content nanoemulsion was probably due to the viscosity effect together with the surfactant's effect on the nasal epithelium.

Rao et al. (Rao et al., 2008a) used  $\beta$ -lactamase (BLM) as the model protein drug and demonstrated that when the drug loaded inside the lipid droplets of o/w nanoemulsion (40 nm), the transportation through MDCK cell monolayer was increased more than 25 times compared to the solution form while the micelle formulation only increased 3 times. It was reported that there was significant increase in transport of BLM through MDCK cell monolayer only when it was loaded inside the inner oil phase of nanoemulsion as compared to BLM aqueous solution. Also, Koga et al. (Koga et al., 2010) reported that

following intraduodenal administration in rats, increase serum concentration of calcein was higher from w/o/w emulsion (300 nm) when calcein was in the inner water phase as compared to when calcein was in the outer water phase of w/o/w emulsion (300nm).

## **2.2 Hypothesis**

The above studies on nanoemulsions imply that loading protein or peptide into the oil phase of nanoemulsions may enhance the absorption due to mucus permeating properties of lipid droplet, protection against enzymatic degradation, reversible opening of tight junctions and transcytosis. Therefore, we hypothesize that loading insulin into the oil phase of nanoemulsions may enhance the intranasal absorption of insulin.

## **2.3 Research Objective**

To develop a nanoemulsion system for intranasal delivery of insulin.

The specific objectives are as follows:

- I. To develop and characterize an o/w nanoemulsions where insulin is loaded inside the oil phase
- II. To evaluate the transport of insulin by such a nanoemulsion through human nasal epithelial cell monolayer *in vitro*
- III. To evaluate the *in vivo* intranasal absorption of insulin such by a nanoemulsion in rats

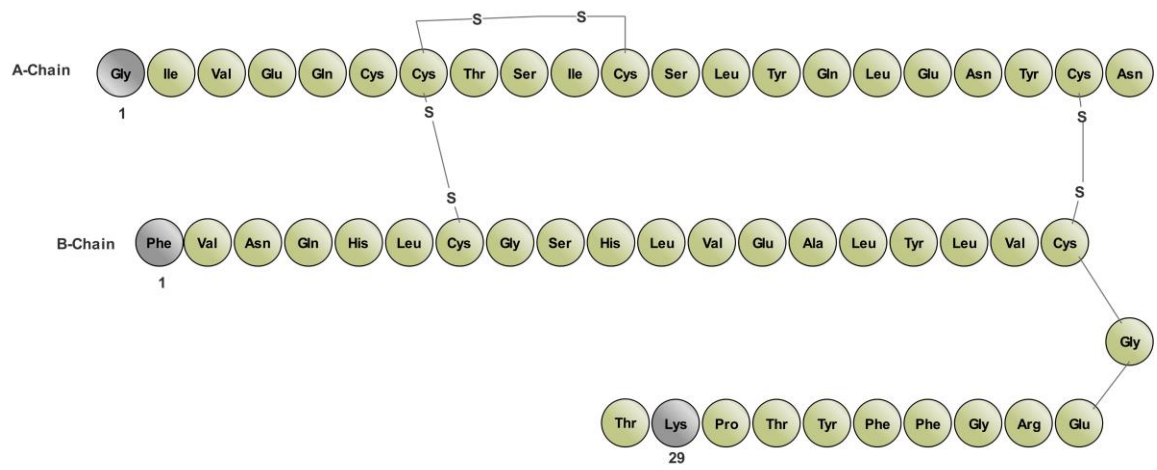


**Fig. 2.** Human insulin structure.

# CHAPTER 3. FITC LABELING OF INSULIN AND TRANSPORT OF FITC-INSULIN CONJUGATES THROUGH MDCK CELL MONOLAYER

## 3.1. Introduction

Fluorescent probes are less expensive, much safer, more stable and much easier to dispose than radioisotopes, and hence they have gained much attention over the last several decades (Rogers, 1997). Fluorescein isothiocyanate (FITC), one of such probes, is widely used for labeling proteins and peptides due to its high detection sensitivity and low molecular size which has potentially low impact on the protein/peptide's biological activity (Ueno and Nagano, 2011).

FITC is an amine reactive fluorescent probe which labels biomolecule by forming a covalent bond between its isothiocyanate group and the primary and secondary amine groups of biomolecules (Banks and Paquette, 1995). FITC (MW 389.4) labeling of human insulin (MW 5807.57) may give mono-, di- and tri- conjugates of insulin since insulin has three primary amine groups (Jacob et al., 2016). Insulin has been previously labeled with FITC and characterized for a number of applications such as protein tracing, protein-protein interaction, assay, analytical detection, microsequencing, drug release study, permeability and cellular uptake study by fluorescence microscopy (Gök and Olgaz, 2004; Hentz et al., 1997; Jacob et al., 2016; Jobbágy and Jobbágy, 1973; P. Li et al., 2016). However, these reported labeling methods are tedious, which takes more than 12 h to produce different conjugates of FITC-Insulin. The reported protocols for labeling are not robust. FITC labeled insulin is also commercially available and has been used by researchers, but is comparatively expensive (P. Li et al., 2016; Ma and Lim, 2003).

Hence, there is still a need to develop an easy, quick and reliable labeling method to prepare different conjugates of FITC labeled insulin. Therefore, one of the aims of the present work is to study the reaction conditions to produce different conjugates of FITC-Insulin and to develop relatively simple and robust method.

The conjugation at different sites affects the biological activity of insulin. The biological activity of the FITC-Insulin conjugates has been reported to differ from that of the native insulin. Hentz et al. studied the biological activity of each conjugate and found that mono labeled FITC-Insulin (tagged at B1 position) had the same biological activity as the native insulin whereas A1 conjugated FITC-Insulin showed 10% decrease in the biological activity and di & tri conjugated FITC-Insulin showed 100% decrease in biological activity as compared to the native insulin (Hentz et al., 1997). The different conjugates may also affect the permeability of insulin due to the difference in molecular weight, hydrophilicity and lipophilicity. To our knowledge, no reports till date have been published regarding the effect of different conjugation on the permeability of FITC-Insulin across a biological membrane. Therefore, the second aim of the present study is to investigate the impact of different FITC conjugates on the hydrophilicity and lipophilicity of insulin and its permeability through a cell monolayer.

### **3.2. Materials**

Human insulin and FITC-Insulin (Human) were purchased from Sigma-Aldrich, Co. (St. Louis, MO, USA). Fluorescein Isothiocyanate, Isomer I, 95% (FITC) was purchased from Alfa Aesar (Tewksbury, MA, USA). PD-10 Sephadex™ G-25 M Columns were purchased from GE Healthcare (Buckinghamshire, UK). Dulbecco's

Modified Eagle's Medium (DMEM), Hyclon TM Hank's 1X Balanced Salt Solution (HBSS), Penicillin-Streptomycin Solution and Trypsin-EDTA Solution were purchased from Fisher Scientific (Middletown, VA, USA). Transwell<sup>®</sup> inserts were purchased from VWR International (Allison Park, PA, USA). Human Insulin ELISA Kit was purchased from Crystal Chem (Elk Grove Village, IL, USA). MDCK cell line was purchased from ATCC<sup>®</sup> (Rockville, MD, USA).

### **3.3. Methods**

#### **3.3.1. FITC Labeling of Human Insulin**

FITC solution in DMSO (5 mg/ml) was added dropwise with gentle stirring to human insulin solution (15 mg/ml) in 0.1 M bicarbonate buffer (pH 9.5) with the molar ratio of FITC:Insulin varying from 0.25:1 to 5:1. The reaction mixture was protected from light and kept at room temperature for 0.5-4 h with continuous slow stirring. Then the reaction mixture was incubated at room temperature for 30 min without stirring. The reaction mixture was then passed through a PD-10 Sephadex<sup>™</sup> G25 column to separate the unbound FITC from insulin and FITC-Insulin conjugates. Phosphate buffer (pH 7.4) was used to elute the mixture from the column and the eluent was collected in 32 fractions (fraction volume – 0.5 ml). Each fraction was analyzed by HPLC to quantify and determine the labeling efficiency. The fractions containing the conjugates were combined together and lyophilized overnight. The lyophilized FITC-labeled insulin powder was stored at -20° C for further use.

### **3.3.2. HPLC Assay**

The HPLC assay of insulin and FITC-Insulin was carried out on an Agilent 1260 system equipped with an Agilent 1260 series UV detector and an Agilent 1220 series fluorescence detector. The analysis conditions were as follows: Column: C18, 5  $\mu$ m, 4.6 X 150 mm; Flow rate: 1 ml/min; Injection volume: 20  $\mu$ l; UV detector wavelength: 220 nm; Fluorescence detector wavelengths: Excitation – 495 nm, Emission – 525 nm; Mobile phase A: Deionized water with 0.1% trifluoroacetic acid (TFA); Mobile phase B: 90% Acetonitrile and 10% deionized water with 0.1 % TFA; Run time: 45 min. Gradient elution was used according to Table 1.

**Table 1.** HPLC gradient elution schedule.

<b>Time (min)</b>	<b>Mobile phase composition</b>
<b>0</b>	85% A + 15% B
<b>15</b>	65% A + 35% B
<b>25</b>	35% A + 65% B
<b>32</b>	35% A + 65% B
<b>33</b>	100% B
<b>43</b>	100% B
<b>44</b>	85% A + 15 % B

**A:** Deionized water with 0.1% TFA

**B:** 90% Acetonitrile and 10% deionized water with 0.1%TFA

### **3.3.3. Lipophilicity and Hydrophilicity Assay of the Conjugates**

The lipophilicity and hydrophilicity of the conjugates were determined by the analysis of the partition coefficient (P). The method described by Griesser et al. (Griesser et al., 2017) was adopted with slight modification. In brief, buffer (pH 7.4) containing 1 mg/ml of either FITC-Insulin conjugates or unlabeled insulin was added to 1-octanol (1:1) and incubated for 8 h at 37° C while shaken at 300 rpm. The samples were centrifuged for 10 min at 9,000 rcf. Aliquots (100 µl) were withdrawn from both the phases and analyzed for absorbance and fluorescence by HPLC. Partition coefficient (P) was calculated as the ratio of the insulin concentration in the octanol phase vs in the aqueous phase.

### **3.3.4. Transport of FITC-labeled Insulin through MDCK Cell Monolayer**

The MDCK cells were grown in 75-cm<sup>2</sup> Corning flasks in DMEM supplemented with 10% (v/v) fetal bovine serum and 1% penicillin-streptomycin solution at 37° C with 5% CO<sub>2</sub> and 95% air with high humidity. The cells were harvested by trypsin-EDTA solution once they reached 80% to 90% confluency, and then seeded on 24 Transwell<sup>®</sup> inserts (1-µm pore size, 0.33-cm<sup>2</sup> growth area) at 6.3 X 10<sup>4</sup> cells/cm<sup>2</sup> with 0.3 ml growth media on the apical side. One ml growth media was added on the basolateral side. The growth media was changed every other day and TEER value was measured. The transport was run on Day 7 once the monolayer had been formed and the TEER value had reached above 300 Ω·cm<sup>2</sup>. The monolayer was washed twice with HBSS and incubated in HBSS for 30 min. Then the transport media on the apical side was replaced by 0.3 ml of unlabeled insulin or FITC-Insulin (2 mg/ml in HBSS). Samples of 200 µl each were

withdrawn from the basolateral side at the predetermined time points until 3 hr. After each withdrawal, same volume of fresh HBSS was added to the basolateral side. The samples containing FITC-Insulin were analyzed for fluorescence by a plate reader (Excitation filter: Blue 475 nm, Emission filter: 500-550 nm) and unlabeled insulin was analyzed by ELISA.

### **3.4. Results & Discussion**

#### **3.4.1. FITC Labeling of Human Insulin**

Human insulin has 51 amino acids divided into two chains: Chain A containing 21 amino acids and Chain B containing 30 amino acid (Fig. 3). There are three primary amine groups in an insulin molecule. Bromer et al. reported that FITC could bind to the three primary amine sites and form mono-, di- and tri-conjugated FITC-Insulin. The order of reactivity of the three primary amines was found to be B1 (Phe) > A1 (Gly) > B29 (Lys) (Bromer et al., 1967).

In the present study, the labeling reaction was conducted at different molar ratios of FITC to Insulin and different reaction time to investigate the impact of these two factors on the products (mono-, di- and tri-conjugated FITC labeled insulin). The reaction mixture after the gel filtration was analyzed by a HPLC connected with an absorbance detector (VWD) and a fluorescence detector (FLD). FITC-labeled insulin gave peaks in both the absorbance and fluorescence chromatograms at around the same retention time, whereas the unlabeled insulin showed a peak only in the absorbance chromatogram but not in the fluorescence chromatogram. Among the 32 fractions from the gel filtration, Fractions 4-9 had the labeled insulin, showing peaks in both chromatograms, and they

were combined. Fig. 4 and Fig. 5 represents the chromatograms of the combined Fractions 4-9 from each reaction as compared to the unreacted insulin (Fig. 5I), the unreacted FITC (Fig. 5H) and the commercial FITC-Insulin (Fig. 4E). Based on the previous reports (Hentz et al., 1997; Jacob et al., 2016), the peaks in the absorbance chromatograms were identified as follows: Peak 1 – unlabeled insulin; Peak 2 – mono-conjugated FITC-Insulin at B1; Peak 3 – mono-conjugated FITC-Insulin at A1; Peak 4 – di-conjugated FITC-Insulin at B1 and A1; Peak 5 – tri-conjugated FITC-Insulin at B1, A1 and B29.

When reaction was carried out for 150 min, different molar ratios of FITC:Insulin produced different conjugates which showed peaks in both detectors as follows (Fig. 4): A) 1:1 molar ratio had unlabeled insulin and it produced mono- and di-conjugates with little quantity of tri-conjugates. B) 2:1 molar ratio produced di- and tri-conjugates where di-conjugate was determined to be in higher amount than tri-conjugate. C) 3:1 molar ratio showed both di- and tri-conjugates where tri-conjugate was determined to be in higher amount than di-conjugate. D & F) Molar ratio 4:1 and 5:1 produced tri-conjugate with very little quantity of di-conjugates.

Molar ratio 0.25:1 with 90 min of reaction time gave mono-conjugated FITC-Insulin along with unlabeled insulin (Fig. 5G). The chromatograms of the products from molar ratio 3:1 FITC-Insulin were similar as that of the commercial FITC-Insulin (Fig. 4C & 4E). Increasing the reaction time for 4:1 to 240 min did not give pure tri-conjugated FITC-Insulin. The products still had small quantity of di-conjugates. Unbound FITC gave peaks at 11 min and 22 min (Fig. 5H) which further confirmed the absence of unbound FITC in the labeled insulin fractions.

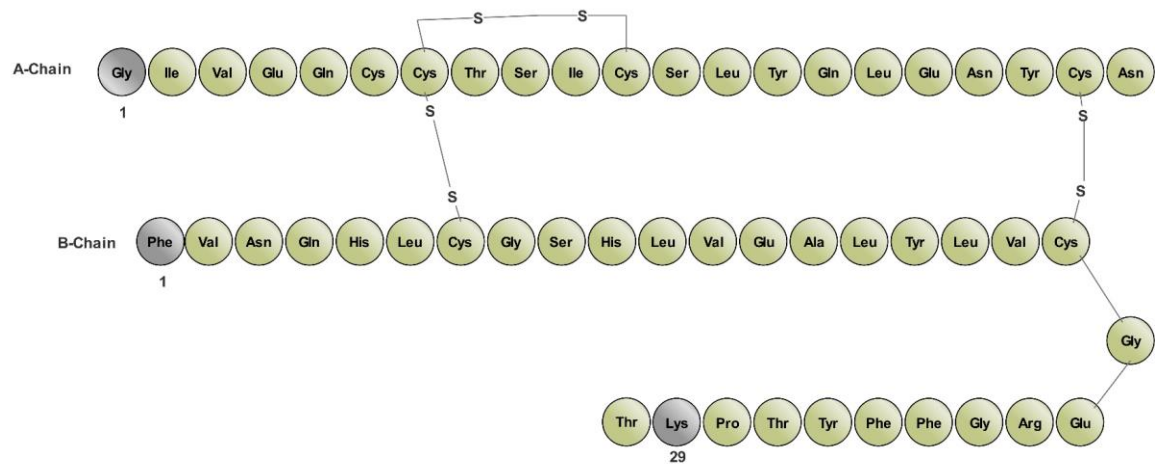


**Fig. 3** Primary structure of human insulin with grey colored circles indicating primary amine sites for FITC labeling.

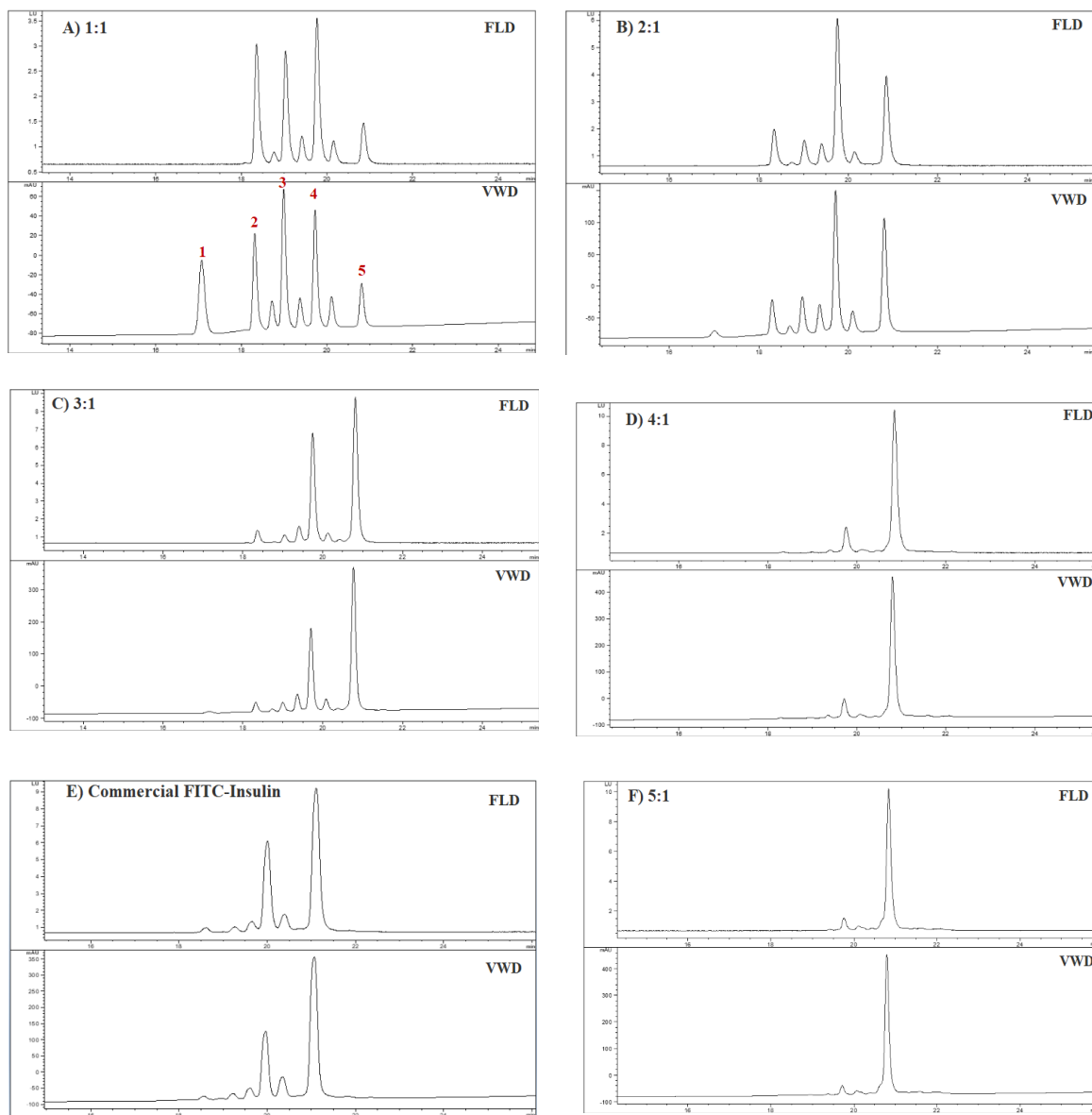


**Fig. 4.** Chromatograms of the FITC labeled insulin. A), B), C), D) and F): with 150 min reaction time and with FITC:Insulin molar ratio of 1:1, 2:1, 3:1, 4:1 and 5:1 respectively, E) Commercial FITC-Insulin.

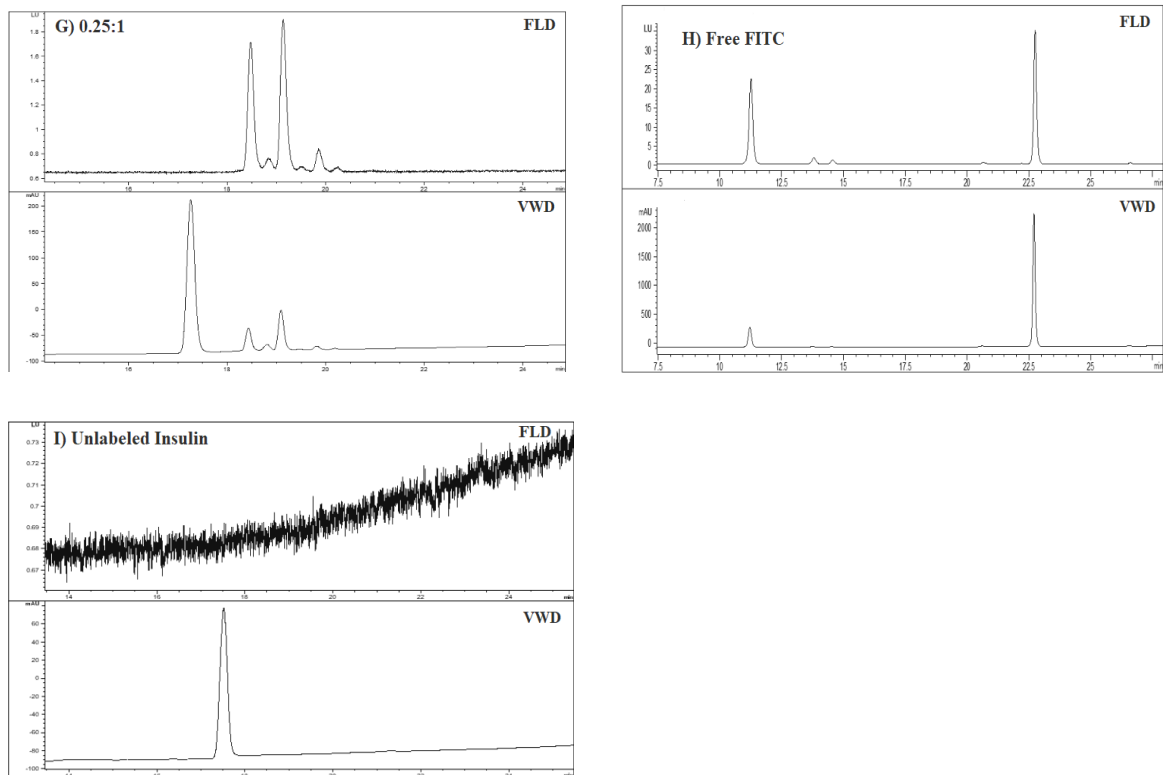


**Fig. 5.** Chromatograms: G) FITC labeled insulin (0.25:1 molar ratio, 90 min reaction time), H) Free FITC, I) Unlabeled Insulin.

### **3.4.2. Lipophilicity and Hydrophilicity of FITC-Insulin**

In order to evaluate the lipophilicity and hydrophilicity of the FITC-labeled insulin, the partition coefficient (P) of the unlabeled insulin, mono- and tri-labeled insulin in the octanol/water system was determined. P value of the unlabeled insulin, mono-conjugate and tri-conjugate was determined to be  $0.07 \pm 0.04$ ,  $0.08 \pm 0.04$  and  $0.12 \pm 0.02$  respectively.

### **3.4.3. Transport of FITC-labeled Insulin through MDCK Cell Monolayer**

MDCK cells have been used as a model cellular barrier for predicting the intestinal epithelial drug transport for many years (Rao et al., 2008a), and take comparatively short time to grow and form tight junction when growing on semi-permeable membranes. Therefore, MDCK cell monolayer was chosen for this study to determine the effect of FITC labeling of insulin on its transport. The mono-conjugated FITC-Insulin, tri-conjugated FITC-Insulin along with the unlabeled insulin were chosen for the transport study. The results are presented in Fig. 6 and Fig. 7.

The unlabeled insulin and mono-conjugated FITC-Insulin showed significantly higher ( $p < 0.05$ ) transport than tri-conjugated FITC-Insulin (Fig. 7). Even though, the partition coefficient value of tri-conjugated FITC-Insulin is higher than mono-conjugate and unlabeled insulin, it showed decreased transport due to the increase in molecular weight (Fig. 6). Molecular weight of tri-conjugate is higher than the mono-conjugate due to the attachment of three FITC molecule to one insulin molecule as compared to mono-conjugate where one FITC molecule is attached to one insulin molecule.

FITC is much more hydrophobic ( $\log P = 5.25$ ) than insulin (Schroeder and Macguidwin, 2010). Mono-conjugated insulin showed slightly higher but not significantly different transport than the unlabeled insulin. Slightly increased permeation could be due to the lipophilicity induced by FITC molecule. Increase in molecular weight of insulin conjugate could be the reason for decreased permeability of tri-conjugated FITC-Insulin through MDCK cell monolayer.

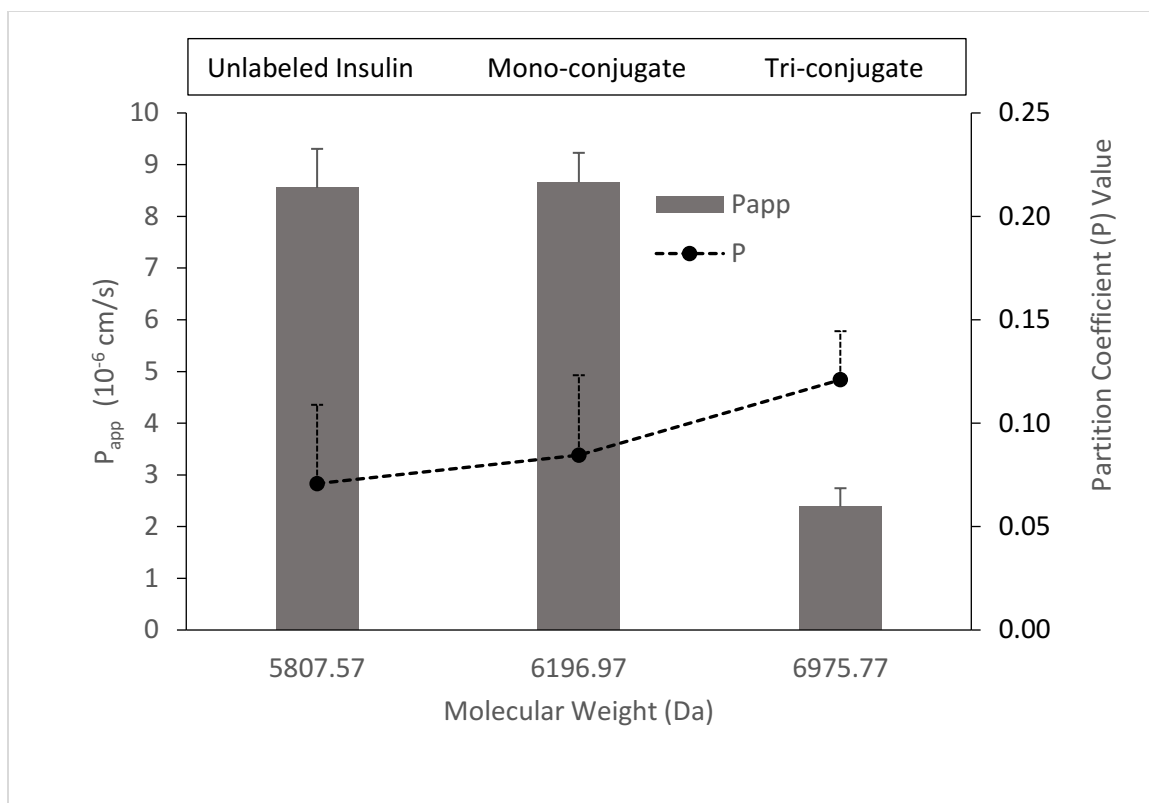


**Fig. 6.** Permeability coefficient ( $P_{app}$ ), molecular weight and partition coefficient (p) value of unlabeled insulin, mono- and tri-conjugates (mean  $\pm$  S.D.,  $n \geq 3$ ).

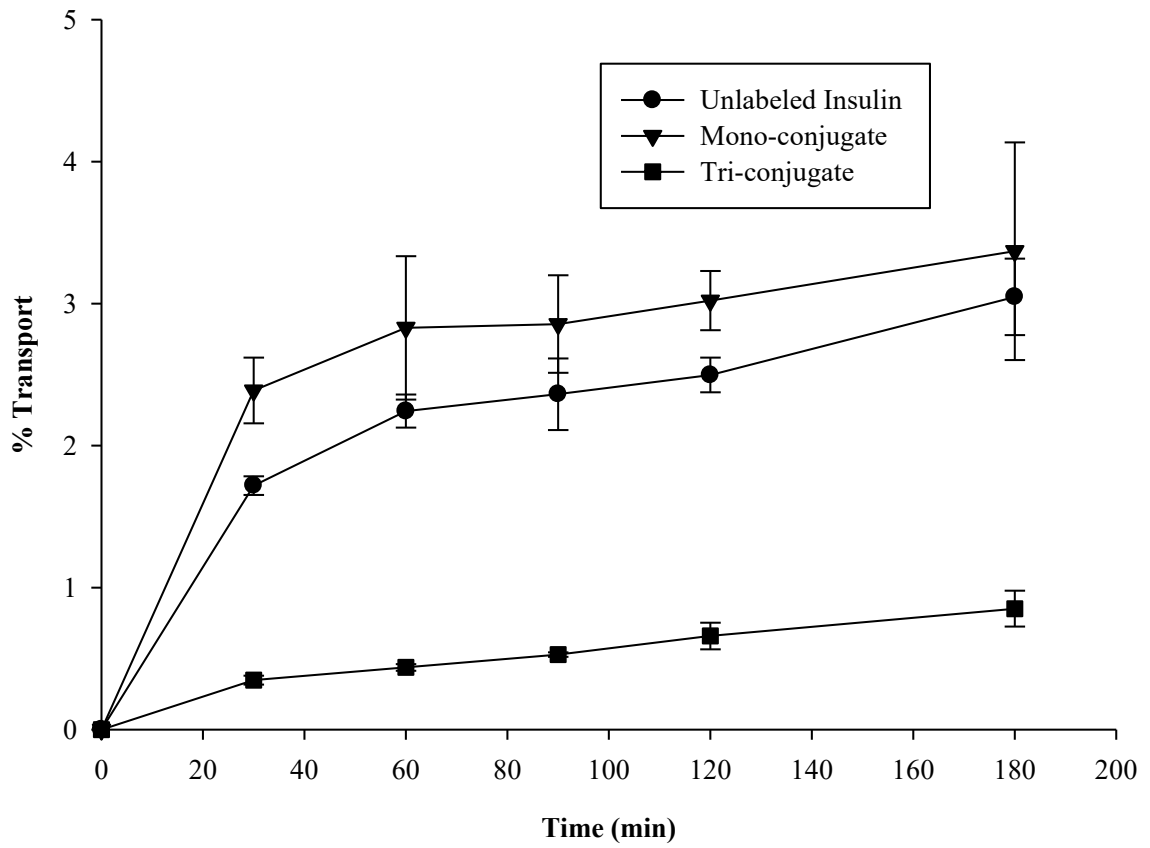


**Fig. 7.** Transport of mono- and tri-conjugated FITC-Insulin and unlabeled insulin through MDCK monolayer, (mean  $\pm$  S.D., n=6).

### **3.5. Conclusion**

A quick, reliable and relatively simple method was developed to synthesize the different conjugates of FITC-Insulin. Extent of conjugation of FITC to insulin did affect the permeability of insulin across cell monolayer.

## CHAPTER 4: FORMULATION DEVELOPMENT AND *IN-VITRO* STUDY

### 4.1. Introduction

Nasal drug delivery has been investigated as an alternative administration route for oral and injection routes. Small molecular compounds and biomacromolecules have been tested for delivery via the nasal route in various formulations. Many formulation approaches have been used to enhance the absorption of macromolecules. The mechanism of absorption enhancement may involve many factors such as local alteration in the membrane structure and modification of its permeability, bioadhesion of the peptide drug to the mucosal surface and lowering of the mucociliary clearance and opening of cellular tight junctions (Marttin et al., 1998, 1995; Shao et al., 1993; Shinichiro et al., 1981). Medium chain fatty acids have been found to enhance the absorption of macromolecules by reversibly opening the tight junctions (P. Li et al., 2016).

The preconcentrate of self-emulsified nanoemulsions are isotropic mixtures of oil(s), surfactant(s) and with or without a co-surfactant(s). When some of these components are mixed in specific ratios, they form oil-in-water nanoemulsion upon addition of buffer or water with droplet size of less than 150 nm. Nanoemulsion systems have been proved to be effective in enhancing the oral bioavailability of many large molecules by providing large surface area for absorption, enhancing permeation due to reversible opening of tight junctions and protecting drugs against enzymatic degradation (AboulFotouh et al., 2018; Hintzen et al., 2014). When loaded into the lipid droplets, the peptide drug can be

protected from enzymatic degradation, can permeate through the mucus gel barrier in a comparatively efficient manner and can be absorbed through transcellular permeation as well as paracellular route (Hintzen et al., 2014; Karamanidou et al., 2015; Rao et al., 2008a).

However, it is difficult to load peptide/protein drugs into lipid due to their hydrophilic nature. This challenge can be overcome by incorporation of hydrophobicity to peptide and protein drugs. Two strategies have been reported in literature to make hydrophilic peptides and proteins more lipophilic and thereby to increase their ability to be incorporated in lipid-based drug delivery systems (Cui et al., 2006; Rao and Shao, 2008; Zhang et al., 2012).

Hydrophobic ion-pairing (HIP) strategy is based on ionic interaction between charged proteins and oppositely charged surfactants. This technique has proved to increase the drug encapsulation efficiency, enhance the permeability and drug transport across membranes and improve oral bioavailability (Anderberg et al., 1993; Aungst and Hussain, 1992; Lee et al., 1991). HIP complexes are reversible in nature and charged protein can easily dissociate in presence of excess of oppositely charged ions (Gaudana et al., 2011). Sodium deoxycholate (SDC) was chosen as HIP complexing agent for the present study. SDC can potentially improve the bioavailability of insulin due to its permeation enhancing properties (Sun et al., 2011). Also, SDC can loosen the tight junctions in the epithelial lining, allowing for paracellular and transcellular transport (Lindmark et al., 1998; Sakai et al., 1997).

Another approach for incorporating hydrophobicity to protein/peptide drug is solid dispersion using anhydrous cosolvent lyophilization of drug and phospholipids.

Phospholipids are surface-active amphiphilic compounds generated naturally in biological membranes by action of phospholipases (Illum et al., 1989). Phospholipid is a vital component of cell membrane with good biocompatibility/biodegradability and low toxicity. They convert within the membrane to normal cell components (Stafford and Dennis, 1987). At present, drug-phospholipid complex has received significant attention due to the amphiphilic characteristic of phospholipid and the convenience, flexibility and versatility of manufacturing process (Khan et al., 2013; Y. Li et al., 2016; Liu et al., 2015). We have selected L- $\alpha$ -phosphatidylcholine (SPC) as complexing agent for this technique as it has ability to fuse into membrane lipids, alter the membrane fluidity and hence enhance the permeation of macromolecules at low concentration without any membrane damage (Illum et al., 1989).

For the elucidation of nasal drug transport mechanism and the investigation of metabolism and toxicity, diverse in vitro models of nasal cell culture systems have been developed. RPMI 2650 cell line, Calu-3 cell line, primary human nasal epithelial cells and passaged human nasal epithelial cells have been widely used in the nasal drug transport study. RPMI2650 is originated from human nasal squamous cell carcinoma of the nasal septum. However, this cell line has the following major drawbacks: no expression of goblet or ciliated cells and no formation of confluent cell monolayers (Kissel and Werner, 1998). The lack of monolayer formation makes this cell line unsuitable for drug transport study. Calu-3 is from a human lung adenocarcinoma. This cell line shows sufficient transepithelial electrical resistance (TEER) values for drug transport studies. Calu-3 cells can develop polarized monolayers and suitable TEER value for transport study but its origin is not from the nasal epithelium (Mathias et al.,

2002). The primary human nasal epithelial cell line is a promising tool for drug permeation study, metabolism study and toxicological study. The nasal cell from primary culture is deemed more appropriate for drug transport studies compared to other cells due to the formation of confluent monolayers and differentiation into goblet and ciliated cells. The human primary nasal cell system has also several limitations including difficulty in obtaining human nasal tissue, possibility of pathogen contamination and donor to donor variability. Serially passaged culture of human nasal epithelial cells has therefore been introduced to overcome these limitations.

Air liquid interface (ALI) and liquid interface (LI) culture of serially passaged human nasal epithelial cells shows musin gene expression and forms confluent monolayer, tight junctions and ciliated cells (Cho et al., 2010). For the nasal absorption of proteins and peptides, the paracellular route of transport which is controlled by tight junction and the enzymatic activity (Sarkar, 1992) of the nasal epithelium are of particular interest. Apart from the structure of the cell line, the characteristic of cell line plays a major role too.

Hence, the passaged cell culture from the primary human epithelial cells is the most suitable *in vitro* cell culture model for the transport study of insulin across nasal epithelium, which was chosen for the present study.

#### **4.2. Materials**

Human insulin (27.5 IU/mg), Kolliphor<sup>®</sup> RH 40, Kolliphor<sup>®</sup> EL and Span<sup>®</sup> 80 were purchased from Sigma-Aldrich, Co. (St. Louis, MO, USA). Olive oil, Soybean oil, Isopropyl palmitate, Span<sup>®</sup> 20, and Brij<sup>®</sup> 97 were purchased from Spectrum Chemical Mfg Corp. (New Brunswick, NJ, USA). Capmul<sup>®</sup> MCM NF, Captex<sup>®</sup> PG-8 NF, Captex<sup>®</sup>

8000 were purchased from Abitec Corporation (Janesville, WI, USA). Tween® 80 was purchased from Amresco, Inc. (Solon, OH, USA). Labrasol and Capryol 90 were purchased from Gattefosse (Paramus, NJ, USA). L- $\alpha$ -phosphatidylcholine (Soy 95%), L- $\alpha$ -Lysophosphatidylcholine and 1,2-Dipalmitoyl-sn-glycero-3-phosphocholine were purchased from Avanti Polar lipids, Inc. (Alabaster, Alabama, USA). Fluorescein isothiocyanate isomer I, Sodium deoxycholate, HEPES, 99% and Glucose anhydrous, 99% were purchased from Alfa Aesar (Tewksbury, MA, USA). Thiazolyl blue tetrazolium bromide, 98% was purchased from Acros Organics (Morris Plains, NJ, USA). Analytical grade Acetonitrile and Methanol were purchased from Fisher Scientific (Fair Lawn, NJ, USA). Dimethyl sulfoxide and Trifluoro acetic acid BDH chemicals (PA, USA). Human nasal epithelial cells (HNEpC), Trypsin inhibitor, 0.04% Trypsin/ 0.03% EDTA and HEPES BSS were purchased from Promo cell (Heidelberg, Germany). Bronchial Epithelial Growth Media (BEGM) was purchased from Lonza (MD, USA). DMEM/F-12 50/50 was purchased from Corning Cellgro (Massachusetts, VA, USA). Penicillin Streptomycin Solution and Transwell inserts were purchased from Corning (Oneonta, New York, USA). Fetal Bovine Serum was purchased from Atlanta Biologicals (Flowery Branch, GA, USA). Mannitol, D-[1-<sup>14</sup>C] and Propranolol, L-[4-<sup>3</sup>H] were purchased from PerkinElmer (Boston, MA, USA).

### **4.3. Methods**

#### **4.3.1. Development and Characterization of Insulin Loaded Self-emulsified Nanoemulsion Formulations**

Specific aims:

- To develop self-emulsified nanoemulsion formulations
- To prepare and characterize lipophilic complexes of insulin
- To evaluate cytotoxicity effects of complexing agents and formulations
- To characterize the insulin complex-loaded nanoemulsion formulations

#### **4.3.2. Development of Self-emulsified Nanoemulsion Formulations**

Different ratios of the long chain (C<sub>18</sub>) and medium chain (C<sub>8</sub>) lipids with nonionic hydrophilic and hydrophobic surfactants (Table 2) were screened to prepared o/w self-emulsified nanoemulsion formulations. The screened o/w nanoemulsion formulations were further investigated to get different droplet size by varying the ratio of lipids to surfactants and/ or the component of the formulation. Ideally, formulations in the size range of 25– 400 nm were prepared. We hypothesize that small lipid droplets have a better chance of getting absorbed intact and thus enhancing the bioavailability of insulin. This study involved phase diagrams, droplet size measurement, polydispersity index, and dilution test.

##### **4.3.2.1 Phase Diagram Construction**

The pseudo ternary phase diagram construction of the nanoemulsion formulation involved a titration method in which the fixed amount of preconcentrate (lipid + surfactant) was diluted with phosphate buffer (pH 7.4) in 10% increments. After each addition of the phosphate buffer, the mixture was shaken in a wrist action shaker at 37° C for 20 min and the mixture was evaluated visually to see whether clear and transparent

nanoemulsion or white emulsion or gel is formed or it has phase separated (Prajapati et al., 2012).

#### **4.3.2.2 Droplet size**

Droplet size and polydispersity index (PDI) were determined by a DelsaNano C droplet size analyzer. The nanoemulsion formulations (diluted 10 times) were taken in a plastic cuvette and were analyzed by the dynamic light scattering technique at 37° C at a scattering angle of 90°, in triplicate (Goddeeris et al., 2006; Prajapati et al., 2012).

#### **4.3.2.3 Dilution test**

The developed nanoemulsion formulations were diluted 5, 10, 25, 50 and 100 times with PBS and the droplet size was measured to determine the effect of dilution on the droplet size.

**Table 2.** List of materials used to develop the self-emulsified nanoemulsion formulations.

<b>Trade Name</b>	<b>Composition</b>
Soybean Oil	Long chain triglyceride (C18)
Isopropyl Palmitate	Ester of isopropyl alcohol and palmitic acid
Capmul MCM NF	Medium chain mono- and diglycerides (C8)
Capmul PG 8	Propylene Glycol Monocaprylate
Olive Oil	Long chain fatty acids (C18)
Captex 8000	Medium chain triglyceride (C8)
Cremophor EL	Polyoxyl 35 castor oil, HLB 12-14
Cremophor RH 40	Polyoxyl 40 hydrogenated castor oil, HLB 14-16
Tween 80	Polyoxyethylene (20) sorbitan monooleate, Nonionic surfactant, HLB -15
Brij 97	Polyoxyethylene 10 oleoyl ether, HLB 12.4
Labrasol	Caprylocaproyl macrogol-8 glycerides EP, HLB - 12
Span 80	Sorbitan monooleate, HLB – 4.3

### 4.3.3. Incorporation of Lipophilicity to Human Insulin Molecule

In order to load insulin into the oil phase, it is necessary to make insulin molecule hydrophobic. Following two methods were used to incorporate the lipophilicity to insulin.

- I. Hydrophobic Ion-pairing
- II. Solid Dispersion

#### 4.3.3.1. Hydrophobic Ion-pairing

Sodium deoxycholate was used for hydrophobic ion-pairing technique. Briefly, various amounts of sodium deoxycholate 1 mg/ml in purified water was added dropwise manner into 5 mg of insulin solution (pH 4.0, 5.0 ml) under magnetic stirring. The solution immediately become cloudy with some precipitation, which was insulin-sodium deoxycholate complex (Ins-SDC) (Sun et al., 2011). The complex was collected by centrifugation at 9000 rcf for 15 min while the free insulin still remained in the supernatant. The resulting pellet was washed with distilled water three times by dispersing and centrifuging. The pellet was then lyophilized and stored at -20° C until further use. The insulin complexation efficiency (CE %) was calculated by measurement of the concentration of free insulin in the supernatant by a high-pressure liquid chromatography (HPLC) method, and the bound insulin fraction was calculated based on the initial amount of insulin added. The insulin CE (%) was calculated by the following equation:

$$\text{CE (\%)} = \frac{A_i - A_f}{A_i} \times 100\% \quad \text{Eq. 1}$$

where,  $A_i$  is initial amount of insulin

$A_f$  is the free insulin present in the supernatant

#### **4.3.3.2. Solid Dispersion**

Soy-L- $\alpha$ -phosphatidylcholine (SPC) was used to prepare the solid dispersion of insulin. To prepare a solvent for co-solubilization of insulin and SPC, 50  $\mu$ l of glacial acetic acid was added to 950  $\mu$ l of dimethyl sulfoxide (DMSO). To this solvent, 40 mg of SPC was added and then sonicated for 10 min to solubilize SPC. Then, 5 mg of FITC-Insulin or human insulin powder was added and sonicated for another 10 min to solubilize insulin. Such prepared clear solution was frozen for 12 h at  $-80^\circ$  C and then lyophilized by a Labconco lyophilizer. The lyophilized Insulin-SPC complex was stored at  $-20^\circ$  C until further use.

#### **4.3.4. Characterization of Insulin Complexes**

The complexes were characterized by differential scanning calorimetry (DSC) and analyzed for partition coefficient in a 1-octanol/aqueous system.

##### **4.3.4.1. Differential Scanning Calorimetry**

The thermal behavior of human insulin, the complexing agents and complexes was analyzed in a modulated differential scanning calorimeter (Q200 DSC; TA Instruments, DE, USA) equipped with a refrigerated cooling accessory. Briefly, 4-5 mg samples were weighed in aluminum pans and were sealed with aluminum lids. For reference, empty sealed aluminum pan was used. The samples were heated from  $-20$  to

190° C at a scan rate of 5° C/min under nitrogen. Each sample was run multiple times and representative thermograms are shown in Fig. 10.

#### 4.3.4.2. Partition Coefficient

Partition coefficient was analyzed by the evaluation of the distribution of insulin in a 1-octanol/aqueous system. To 5 ml of aqueous phase (phosphate-buffered saline, pH 7.4), 5 mg of insulin powder or insulin complex was added. Five ml of 1-octanol was added to the resultant mixture and incubated at 37° C while shaking at 300 rpm for 12 h. The two phases were separated by centrifugation at 9,000 rcf for 10 min. Aliquots of 200 µl of the octanol and aqueous phases were diluted with 800 µl of methanol containing 0.1% (v/v) trifluoroacetic acid (TFA). The insulin concentration in both phases was determined by HPLC. The partition coefficient was calculated by the following equation,

$$PC = \frac{\text{Insulin concentration in octanol phase}}{\text{Insulin concentration in aqueous phase}} \quad \text{Eq. 2}$$

#### 4.3.5. Cytotoxic Effect of Nanoemulsion Components and Complexing Agents on Human Nasal Epithelial Cells (HNEpC)

Viable cells with active metabolism convert MTT (3-(4, 5-dimethylthiazol-2-yl)-2, 5-diphenyltetrazolium bromide) into a purple-colored formazan product with an absorbance near 560 nm. When cells die, they lose the ability to convert MTT into formazan, thus the color formation serves as a useful and convenient marker of only viable cells (Riss et al., 2004). The quantity of formazan (presumably directly

proportional to the number of viable cells) is measured by the absorbance at 560 nm (Rao et al., 2008a).

The cytotoxicity of complexing agents and nanoemulsion components on the human nasal epithelial cells (HNEpC) was evaluated by the MTT colorimetric assay. Briefly, 15000 cells in 200  $\mu$ l BEGM were seeded into each well of the 96-well plates and incubated (37° C, 5% CO<sub>2</sub>). After 48 h culture, the cells were further incubated with 200  $\mu$ l of BEGM containing either different concentration of the complexing agents or formulation components for 3 h. Then, the incubation medium was aspirated and the cells were washed with HBSS. Fresh BEGM (180  $\mu$ l) and 20  $\mu$ l of MTT solution prepared in BEGM (4.0 mg/ml) were added to each well. After 3 h of incubation, the supernatant was discarded and formazan crystals were dissolved in 200  $\mu$ l DMSO followed by vigorous mixing for 15 min. The absorbance was determined by a microplate reader at 560 nm. The percent viability of the cells was determined by following equation,

$$\text{Cell viability} = 100\% - \{[(AC-AT)/AC] \times 100\% \} \quad \text{Eq. 3}$$

where, AC is the absorbance of the control well and AT is the absorbance of the treated well.

#### **4.3.6. Preparation of Insulin Loaded Self-emulsified Nanoemulsions**

Insulin-SDC, Insulin-SPC, and FITC-Insulin-SPC complexes were solubilized or dispersed in the oil phase of the nanoemulsion formulations. One g of oil mixture was

added to the lyophilized complexes and was shaken at 200 rpm for 2 h at 37°C. If the complex was not completely dispersed or solubilized, further amount of oil was added until it became either a clear oily solution or homogenous dispersion.

Required amount of surfactant according to the formulation was added to complex-loaded oil mixture and was kept for shaking for 1 h at 300 rpm and 37°C. One g of the complex-loaded preconcentrate was diluted further with PBS to form nanoemulsion and was shaken for 1 h at 300 rpm and 37°C.

The complex-loaded nanoemulsion formulations were characterized for droplet size, polydispersity index, and leakage of insulin from the oil phase to the aqueous phase.

#### **4.3.6.1. Droplet Size**

The nanoemulsion with insulin loaded in the oil phase were evaluated for droplet size by a DelsaNano C droplet size analyzer and the droplet size of the blank nanoemulsions with insulin solubilized in aqueous phase was also analyzed.

#### **4.3.6.2. Leakage of Insulin from the Oil Phase**

The leakage of the insulin from the oil phase into the aqueous phase of the nanoemulsion was studied by the membrane filtration method (Khatri and Shao, 2017a). Ten ml of the nanoemulsion was added to a Centriprep® 30K tube and centrifuged at 1,500 g for 10 min. Insulin concentration in the filtrate collected after centrifugation was

analyzed by HPLC and compared to the insulin concentration in the nanoemulsion before centrifugation to calculate the leakage of insulin from the oil phase.

#### **4.3.7. Transport of Insulin by Nanoemulsion through Human Nasal Epithelial Cell Monolayer**

##### **Specific aim:**

- To study the transport of insulin by the nanoemulsion system through human nasal epithelial cell monolayer.

##### **4.3.7.1. HNEpC Transport Study**

Briefly, cryovial from the liquid nitrogen container was removed and immediately placed on dry ice – even for short transportation. Under a laminar flow bench, cap of the cryovial was twisted quarter turn to release the pressure, then re-tightened. Vial was then immersed into a water bath (37° C) just up to the screw cap for 2 min. It was ensured that no water entered the thread of the screw cap. The vial was disinfected with 70% v/v ethanol under a laminar flow bench. The cells were seeded at 10,000 cells/cm<sup>2</sup> in a cell culture flask containing the pre-warmed growth medium (BEGM). The flask was placed in an incubator at 37° C with 95% humidified air and 5% CO<sub>2</sub>. The culture media was replaced after 16-24 h and then every other day (Schmidt et al., 1998).

Once the cells reached 70-80 % confluency, the cells were detached by the detach kit from Promocell and cells were further seeded on a Transwell inserts at a density of

$5 \times 10^5$  cells/cm<sup>2</sup>. The apical and basolateral side of the transwells were filled with 0.3 ml and 1.0 ml of cell culture media respectively. Media of both sides were changed after the first 24 h and then every other day. The remaining detached cells were further subcultured for the next passage at a density of 10,000 cells/cm<sup>2</sup>, and the growth medium was changed every other day.

The transepithelial electrical resistance (TEER) value of the transwell inserts was measured by an EVOM voltohmmeter device, and the transwell inserts with TEER values higher than 300  $\Omega \cdot \text{cm}^2$  were chosen for the transport study. Transport medium was HBSS (Hank's Balanced Salt Solution) supplemented with 15 mM glucose and 15 mM HEPES buffer, pH 7.4 (Lin et al., 2007, 2005). Prior to each experiment, the monolayers were washed with a pre-warmed transport medium, and were allowed to equilibrate for 20 min in the incubator with 0.3 ml of transport media on the donor side and 1.0 ml of transport media in receiver side. Then, the transport media in donor side was replaced with 0.3 ml of formulations prepared in transport medium to evaluate the permeation from apical to basolateral direction. Aliquots of 200  $\mu\text{l}$  were withdrawn from the basolateral compartment at pre-determined time points (30, 60, 90, 120 and 180 min). Aliquots were assayed for fluorescence using plate reader to quantify the permeated FITC labeled insulin. The % transport was calculated.

***In vitro* transport and monolayer integrity studies were carried out for following formulations:**

- FITC-Insulin-SPC complex loaded in oil phase of nanoemulsion
- FITC-Inulin solubilized in aqueous phase (transport media) of blank nanoemulsion

- FITC-Insulin-SPC complex dispersed in transport media, pH 7.4
- FITC-Insulin Solution in transport media, pH 7.4

#### **4.3.7.2. HNEpC Monolayer Integrity Study**

Propranolol, L-[4-<sup>3</sup>H] and Mannitol, D-[1-<sup>14</sup>C] were used as transcellular and paracellular markers, respectively (Rao et al., 2008a). HNEpC monolayer was formed as described in the transport study (previous section 4.3.7.1.). Once the TEER values were higher than 300  $\Omega \cdot \text{cm}^2$ , 0.3 ml of formulations prepared with transport media containing 0.5  $\mu\text{Ci/ml}$  of Propranolol and 0.03  $\mu\text{Ci/ml}$  of Mannitol were added on the donor side and 1 ml of transport media was added on the basolateral side of the transwell inserts. The monolayer was incubated for 3 h at 37°C with 5% CO<sub>2</sub> and 95% air. Aliquots of 200  $\mu\text{l}$  were withdrawn from the basolateral compartment at pre-determined time points (30, 60, 90, 120 and 180 min) and replaced with fresh 200  $\mu\text{l}$  of transport media. The samples were assayed for Propranolol, L-[4-<sup>3</sup>H] and Mannitol, D-[1-<sup>14</sup>C] by radioactivity measurement. Aliquoted 100  $\mu\text{l}$  samples were mixed with 3 ml of scintillation cocktail and the disintegrations per min (dpm) was counted by a Tri-carb Liquid Scintillation Analyzer Model B3110 TR (PerkinElmer, Shelton, CT, USA).

#### **4.3.8. Data Analysis**

The values were expressed as mean  $\pm$  S.D. Statistical analysis was performed by student's t-test. A value of  $p < 0.05$  was considered to be statistically significant.

## 4.4. Results

### 4.4.1. Formulation Development

Self-emulsified nanoemulsions are thermodynamically stable, single-phase, translucent or opalescent liquid systems composed of an oil or oil mixture and a surfactant or surfactant mixture which forms oil in water nanoemulsion upon addition of water with gentle agitation.

Nanoemulsion formulations were developed by first screening six oils and six surfactants listed in Table 2. in various ratios with PBS. Formulations which formed clear or translucent systems with droplet size less than 150 nm were characterized as nanoemulsions. Phase diagrams with nanoemulsion regions were considered for formulation development study.

In our study, medium chain lipids capmul MCM and captex 8000 with cremophor RH40 and cremophor EL showed a clear (nanoemulsion) region (Fig. 8). To increase the nanoemulsion region these two oils were mixed in various ratios and were evaluated for nanoemulsion formation with cremophor RH40 as surfactant and PBS (Table 3.). Formulations NE-3, NE-5, NE-6, NE-8, and NE-9 showed droplet size less than 50 nm when diluted 10 times with PBS. Whereas, formulations NE-1, NE-2, NE-4 and NE-7 showed droplet size higher than 100 nm with 10 times dilution. Nanoemulsions (NE-1 to NE-9) were further investigated for effect of dilution on droplet size and results are shown in Table 4. It was observed that formulations with droplet size higher than 100 nm had effect of dilution on droplet size. Whereas, formulations with droplet size less than 50 nm had no effect of dilution on droplet size. These formulations were further

evaluated for toxicity on human nasal epithelial cells to select a nanoemulsion with least possible toxic effects on cells.

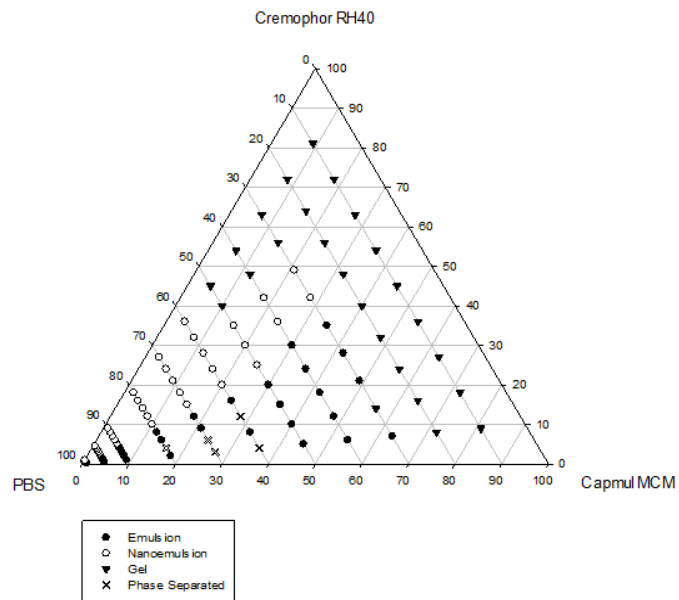
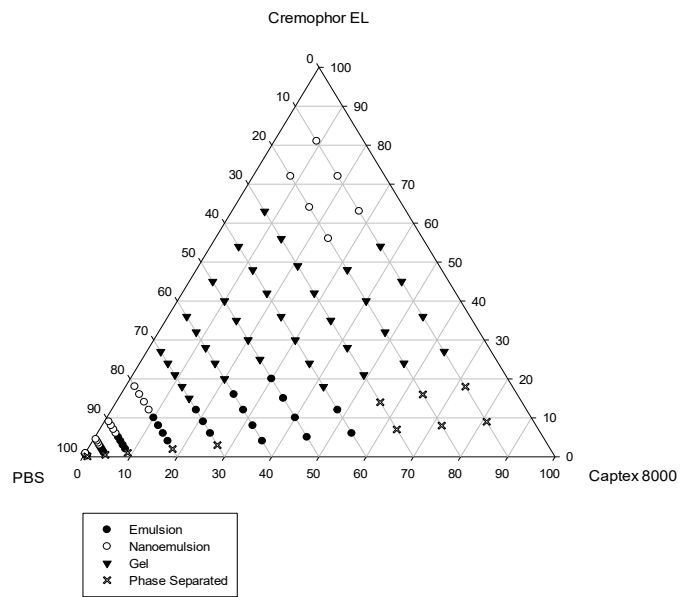


**Fig. 8.** Phase diagram of Captex 8000: Cremophor EL: PBS and Capmul MCM:  
Cremophor RH40: PBS.

**Table 3.** Formulation composition, droplet size and polydispersity index (PDI) at 10 times dilution with PBS (mean  $\pm$  S.D., n=3).

<b>Formulation Name</b>	<b>Capmul MCM: Captex 8000</b>	<b>Oil Mix: Cremophor RH40</b>	<b>Droplet Size (nm)</b>	<b>PDI</b>
NE-1	7:3	7:3	714.3 $\pm$ 45.0	0.374 $\pm$ 0.04
NE-2	7:3	6:4	447.3 $\pm$ 89.6	0.366 $\pm$ 0.06
NE-3	7:3	5:5	28.8 $\pm$ 4.1	0.244 $\pm$ 0.16
NE-4	6:4	7:3	543.7 $\pm$ 432.0	0.356 $\pm$ 0.0.
NE-5	6:4	6:4	33.8 $\pm$ 1.8	0.212 $\pm$ 0.06
NE-6	6:4	5:5	35.3 $\pm$ 9.9	0.139 $\pm$ 0.13
NE-7	5:5	7:3	115.7 $\pm$ 133.4	0.285 $\pm$ 0.13
NE-8	5:5	6:4	36.1 $\pm$ 3.4	0.243 $\pm$ 0.04
NE-9	5:5	5:5	29.5 $\pm$ 1.7	0.208 $\pm$ 0.06

**Table 4.** Effect of dilution with PBS on droplet size of the formulations (mean  $\pm$  S.D., n=3).

Formulation Name	Dilution Times with PBS			
	10	25	50	100
NE-1	714.3 $\pm$ 45.0	387.8 $\pm$ 17.7	151.5 $\pm$ 12.2	42.4 $\pm$ 2.9
NE-2	447.3 $\pm$ 89.6	148.1 $\pm$ 14.8	31.5 $\pm$ 1.5	32.7 $\pm$ 0.5
NE-3	28.8 $\pm$ 4.1	26.4 $\pm$ 2.1	24.5 $\pm$ 0.6	25.9 $\pm$ 0.4
NE-4	543.7 $\pm$ 432.0	78.8 $\pm$ 24.4	60.5 $\pm$ 24.8	44.4 $\pm$ 2.2
NE-5	33.8 $\pm$ 1.8	31.7 $\pm$ 2.3	31.5 $\pm$ 3.5	31.9 $\pm$ 3.4
NE-6	35.3 $\pm$ 9.9	27.4 $\pm$ 1.0	28.7 $\pm$ 1.0	29.0 $\pm$ 0.5
NE-7	115.7 $\pm$ 133.4	148.7 $\pm$ 69.4	90.1 $\pm$ 19.4	78.1 $\pm$ 3.6
NE-8	36.1 $\pm$ 3.4	35.8 $\pm$ 4.3	36.1 $\pm$ 1.9	36.7 $\pm$ 1.6
NE-9	29.47 $\pm$ 1.70	30.97 $\pm$ 3.64	30.5 $\pm$ 1.2	30.4 $\pm$ 1.0

#### **4.4.2. Preparation of Insulin Complexes**

Insulin being a hydrophilic molecule, has very poor solubility in hydrophobic organic solvents and lipids. However, with hydrophobic ion-pairing and solid dispersion methods, it is possible to load insulin into lipid-based drug delivery systems.

##### **4.4.2.1. Hydrophobic Ion-pairing**

Insulin has six basic groups and six acidic groups with an isoelectric point of 5.35 – 5.45 (Dai and Dong, 2007). It is positively charged below the isoelectric point (due to two histidine, one lysine, one arginine, and two N-terminal amino acid residues). Sodium deoxycholate (SDC) being an anionic surfactant (pKa 6.3) forms a complex (Ins-SDC) with insulin at pH 4.0 by ionic interaction. As shown in Fig. 9, increasing the molar ratio of SDC:Insulin increased the complexation efficiency (CE). Maximum CE was achieved when the molar ratio was 6:1, as SDC has one negative charge and insulin can have six positive charges when all the basic groups are ionized. Therefore, 6:1 molar ratio of SDC:Insulin was used for further studies. These results were in agreement with previously published data by Sun et al. (Sun et al., 2011).

Sun et al. studied the net surface charge of Ins-SDC complex and reported that it was positive up to molar ratio 6:1 due to surplus positively charged insulin and it became nearly zero for molar ratio 6:1. Further addition of sodium deoxycholate above 6:1 molar ratio gave negative net surface charge due to higher amount of SDC present in complex (Sun et al., 2011).

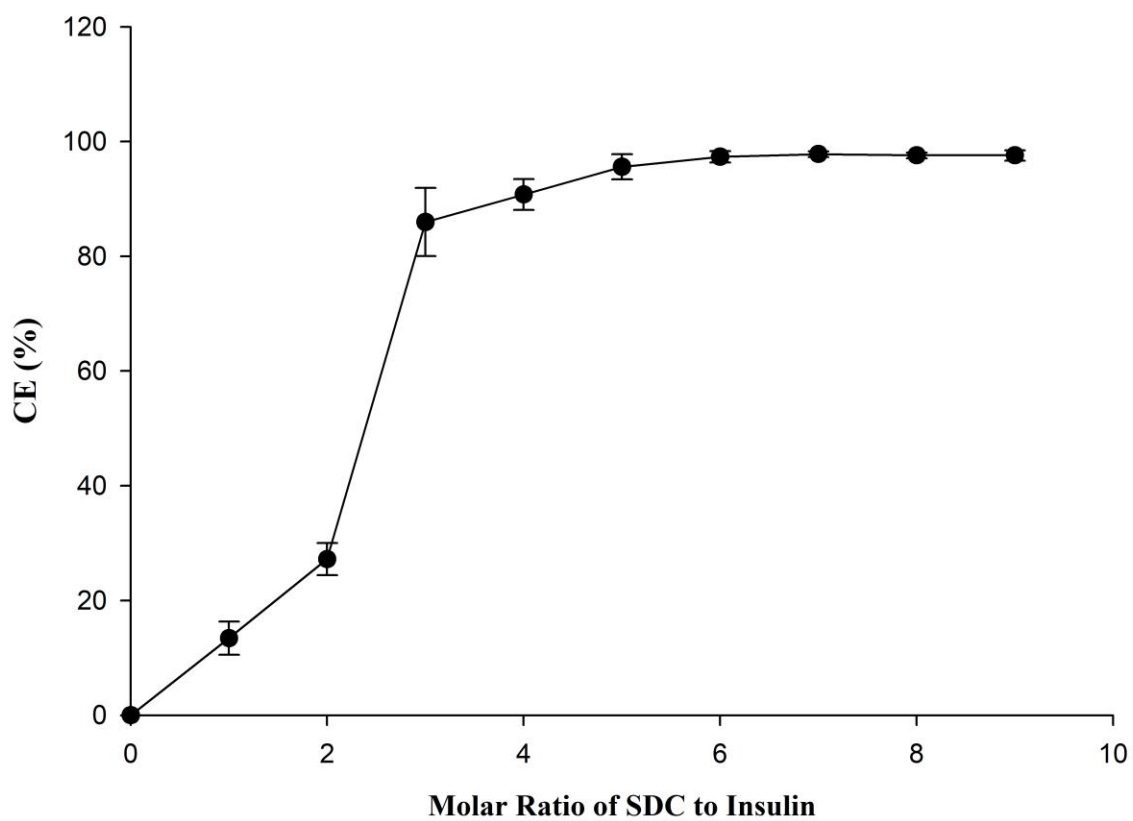


**Fig. 9.** Complexation efficiency (%) vs molar ratio of sodium deoxycholate (SDC) to Insulin (mean  $\pm$  S.D., n=3).

#### **4.4.2.2. Solid Dispersion**

SPC, being an amphiphilic molecule, has been widely used to improve the solubility and bioavailability of drugs (Xie et al., 2017). Ins-SPC complex was prepared by anhydrous co-solvent lyophilization process. Both insulin and SPC were dissolved in acidified DMSO, and then lyophilized. Since DMSO is an aprotic polar solvent with great biocompatibility and dissolvable capacity for many substances, it has been generally utilized as protein dissolving agent during the process of supercritical antisolvent precipitation (Winters et al., 1996).

Increasing the molar ratio of SPC to insulin increases the transmittance of organic solvent system gradually. Cui et. al. studied the transmittance of the Ins-SPC complex solubilized organic solvent systems and observed that transmittance of the system reached to 100% when molar ratio 60:1 of SPC:Insulin was used which indicated that insulin was completely solubilized in organic solvent (Cui et al., 2006). Therefore, in order to achieve maximum lipophilicity, molar ratio of 60:1 and weight ratio of 8:1 of SPC:Insulin was used to prepare the complex. Porous complex was obtained when the complex solution was lyophilized at  $-54^{\circ}\text{C}$  for 12 h. It formed a thin and dry gel like waterless layer which was further evaluated for complex formation and was loaded into the nanoemulsion system.

#### **4.4.3. Characterization of Insulin Complexes**

##### **4.4.3.1. Differential Scanning Calorimetry**

The results of differential scanning calorimetry are presented in Fig. 10. Thermograms of insulin showed no specific events, indicating that insulin was in

amorphous form. Whereas, SDC showed a sharp exothermic peak around 175° C and two broad tiny peaks around 120° C and 140° C, indicating that SDC was in crystalline form. However, Ins-SPC complex thermogram indicates that the complex was in amorphous form and SDC lost its crystalline characteristics when complexed with insulin.

SPC thermogram showed a wide exothermic peak around 160 °C, which might be due to degradation. Ins-SPC complex was observed to be amorphous with Tg of 100 °C.

The above DSC results confirmed that complexes were formed and both the complexes were in amorphous form.

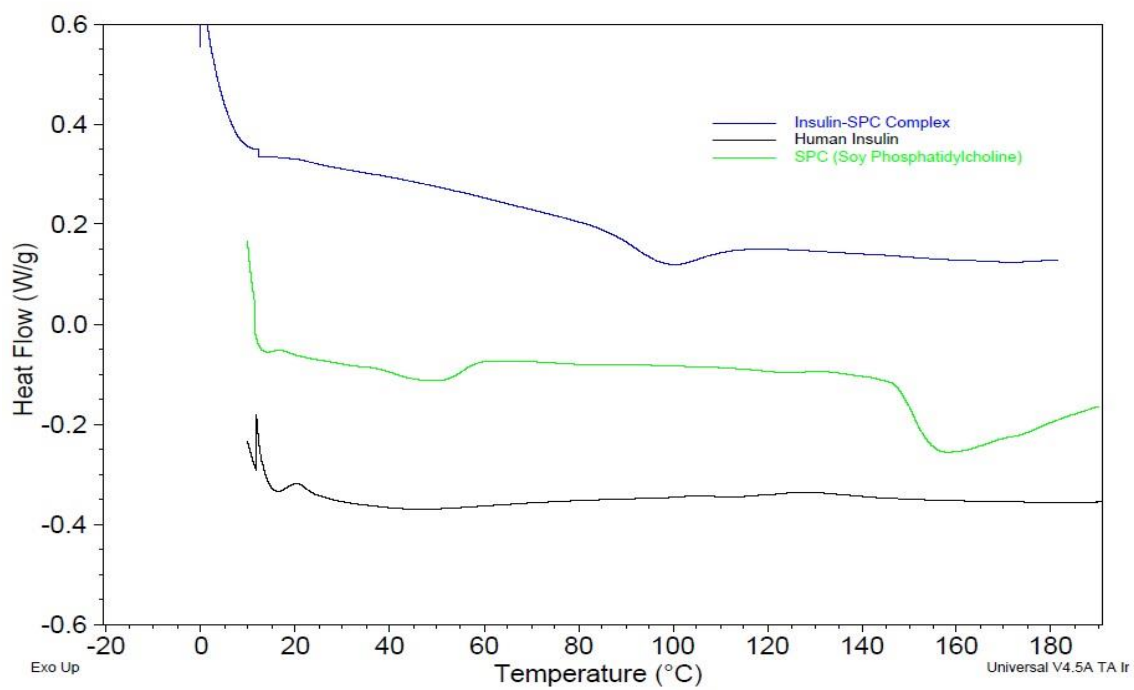
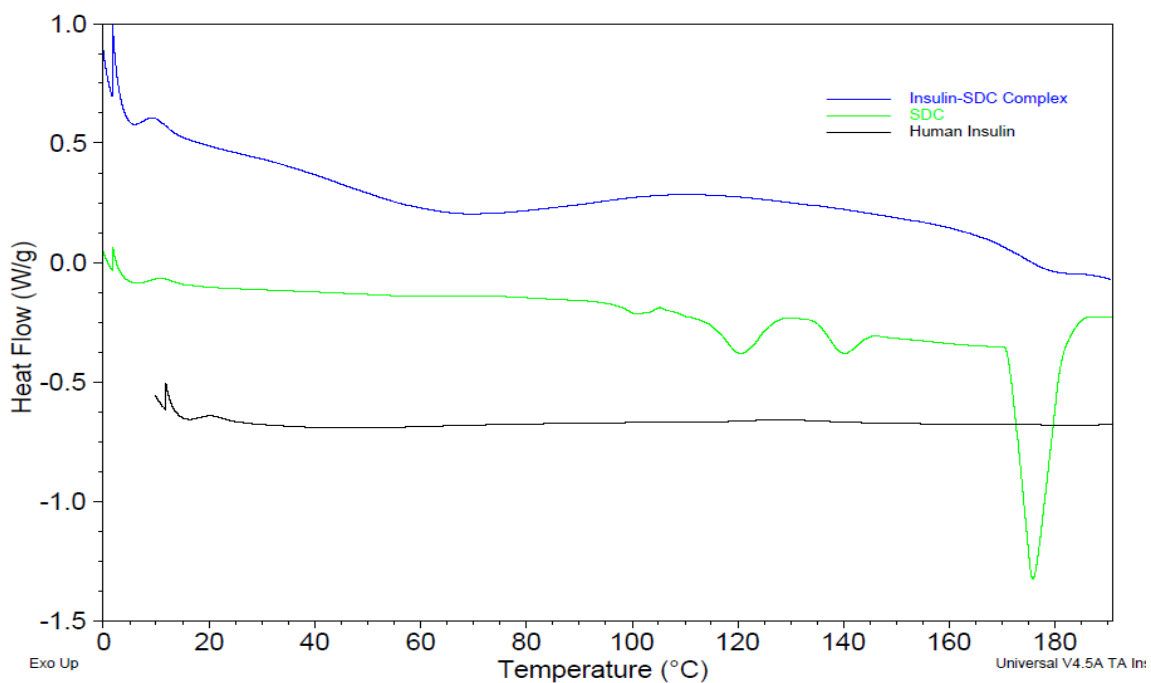


**Fig. 10.** Representative thermograms of insulin, complexing agents (SDC and SPC), Ins-SDC complex and Ins-SPC complex.

#### 4.4.3.2. Partition Coefficient

In order to determine the incorporation of lipophilicity to the insulin molecule, the partition coefficient of insulin, Ins-SDC complex and Ins-SPC complex in 1-Octanol/Aqueous system was determined. The partition coefficient of insulin, Ins-SPC and Ins-SDC complex was determined to be  $0.07 \pm 0.04$ ,  $0.73 \pm 0.15$ , and  $0.53 \pm 0.21$ , (mean  $\pm$  S.D., n=3) respectively (Fig. 11). The two complexes increased the partition coefficient about 8-10 times. Such significant increase in partition coefficient values indicated that lipophilic complexes of insulin were formed.

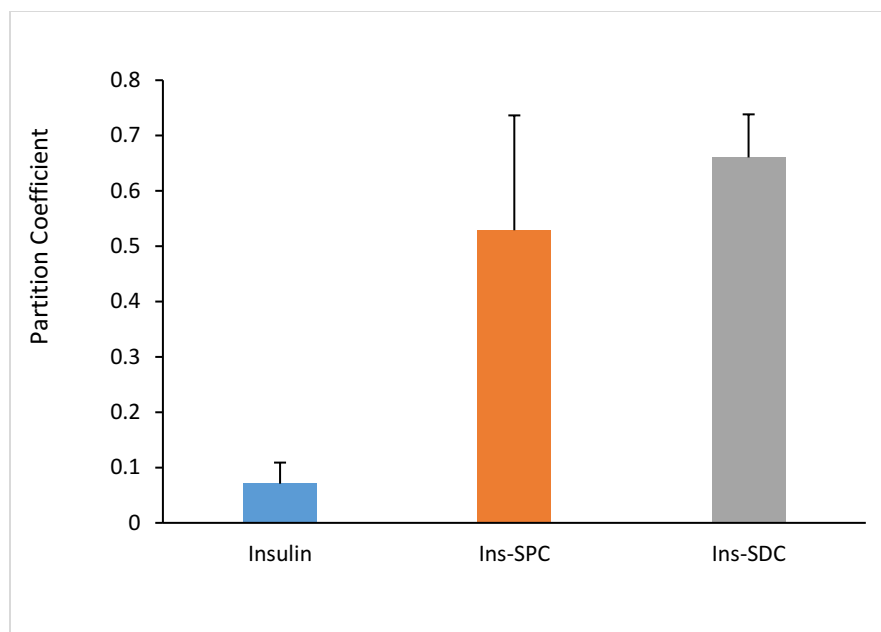


**Fig. 11.** Partition coefficient of insulin and insulin complexes (mean  $\pm$  S.D., n=3).

#### **4.4.4. Cytotoxicity of Formulation Components and Complexing Agents on Human Nasal Epithelial Cells (HNEpC)**

In order to develop a formulation with least toxicity effect on human nasal membrane, cytotoxicity of the complexing agents, surfactant and formulation on human nasal epithelial cells was carried out by MTT assay.

SDC had an effect on the viability of human nasal epithelial cells. As shown in Fig. 12A, increase in concentration of SDC from 0.1% to 10% decreased the viability of HNEpC. At lowest concentration of 0.1% of SDC, the viability was observed to be  $43.59\% \pm 6.91\%$ .

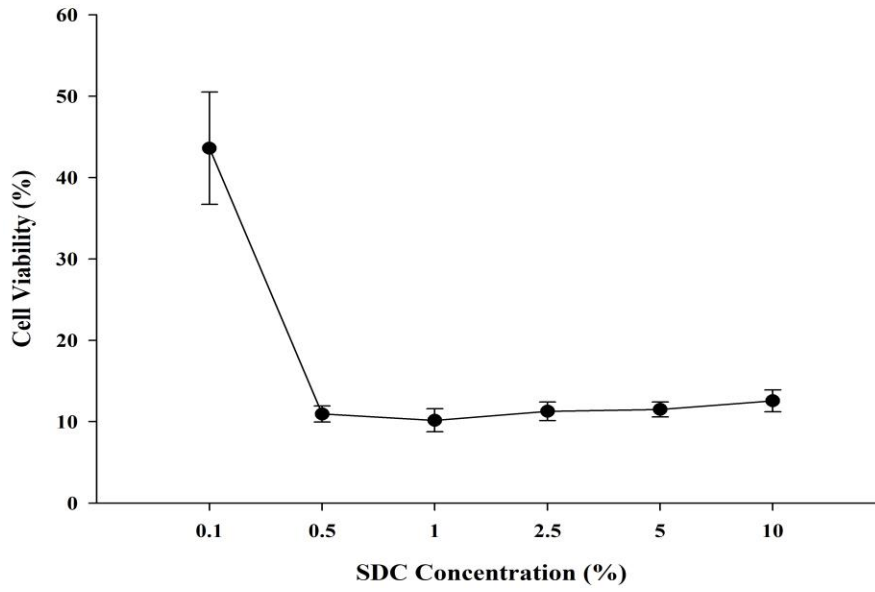
SPC did not have any significant effect on viability of HNEpC. Concentration of 0.1% to 10% of SPC were used for the cytotoxicity study and it was observed that even at 10% concentration, the cell viability was  $88.90\% \pm 15.12\%$  (Fig. 12B). It was concluded from this study that SPC was much safer compared to SDC as it showed no toxic effect on the cells. Hence further experiments were carried out with SPC as the complexing agent.

Surfactant Cremophor RH40 shows concentration-dependent effect on the cell viability. As shown in Fig. 13, when the Cremophor RH40 concentration increased from 0.1% to 10%, the cell viability decreased from 100% to about 40%. The cell viability was  $81.36\% \pm 18.51\%$  at 1% Cremophor RH40. Hence, cremophor RH 40 was found to be least toxic below concentration of 1%.

Formulations NE-1 to NE-9 were evaluated at different dilutions for cytotoxicity, and the results are depicted in Fig. 14. The viability of HNEpC increased as the number of dilutions increased. All the formulations were observed to be toxic at 10- and 25-times dilutions with PBS (Fig. 14A), resulting in about 10% cell viability. When the formulations were diluted 50 times, NE-8 and NE-9 resulted in over 80% cell viability, whereas, the other formulations exhibited lower than 45% cell viability (Fig. 14B). At 50 times dilution, RH 40 concentration was 1% or lower for all formulations. Since RH40 alone showed more than 80% viability at 1% or lower concentration, this cytotoxicity effect (less than 5% viability) could be due to the toxic effect of lipids. Capmul MCM and Captex 8000 were used in various ratios to prepare the lipid mixture. Capmul MCM concentration decreased in the formulations from NE-1 to NE-9, and the cell viability had increased from NE-1 to NE-9. Similar trend was observed at 100 times dilution.

Therefore, NE-8 and NE-9 were considered to be less toxic as compared to other formulations and were used for further studies.

### A. Cytotoxicity of SDC



### B. Cytotoxicity of SPC

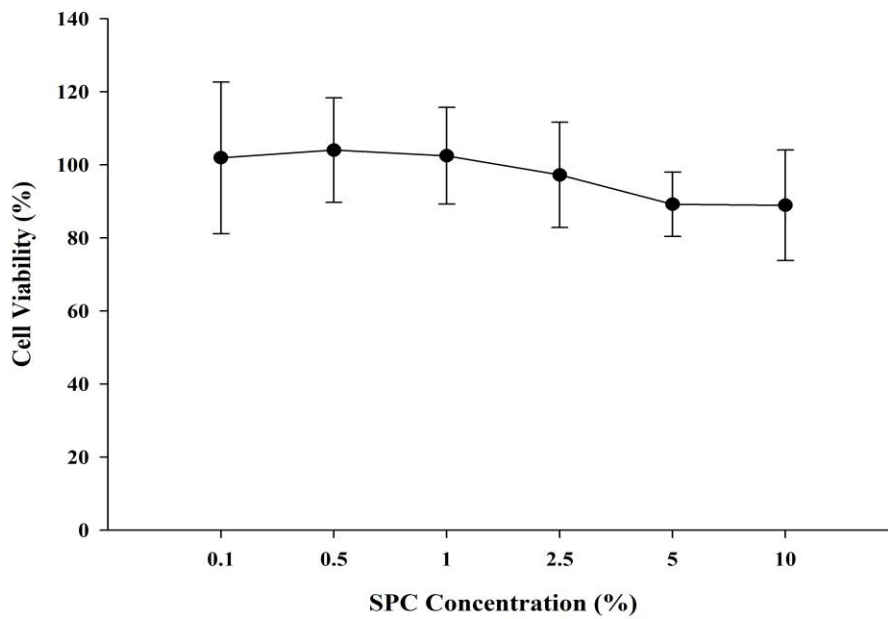


**Fig. 12.** Effect of the complexing agents A) SDC and B) SPC on the viability of human nasal epithelial cells after 3 h exposure *in vitro* (mean  $\pm$  S.D., n=6).

### Cytotoxicity of Cremophor RH40

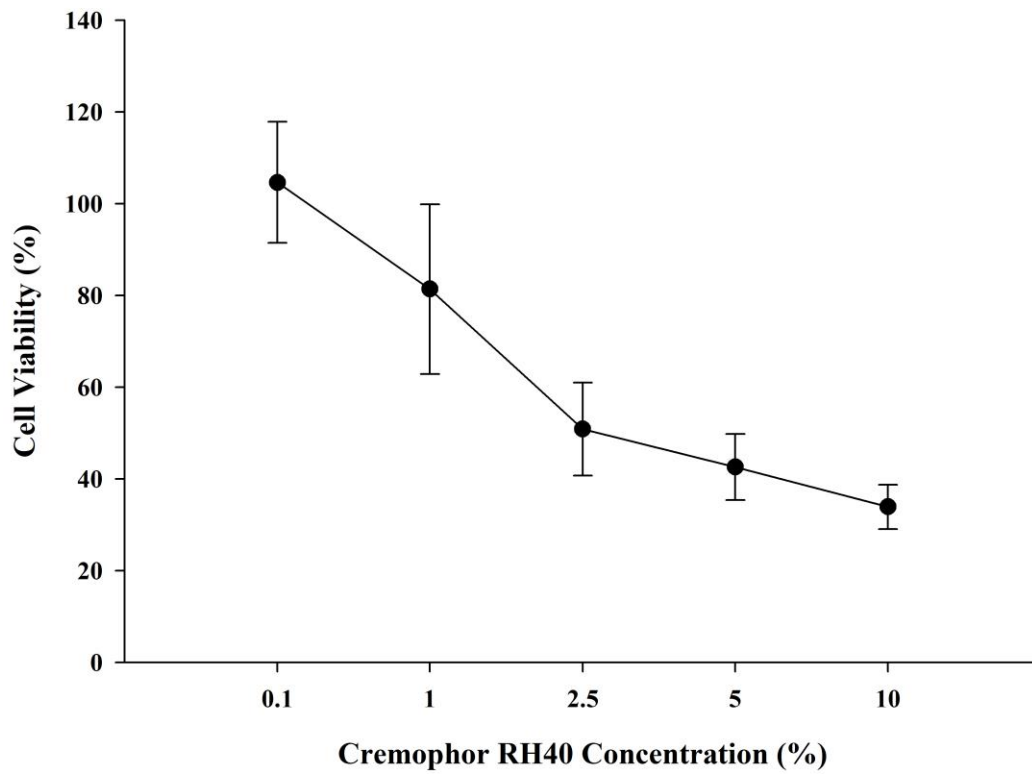
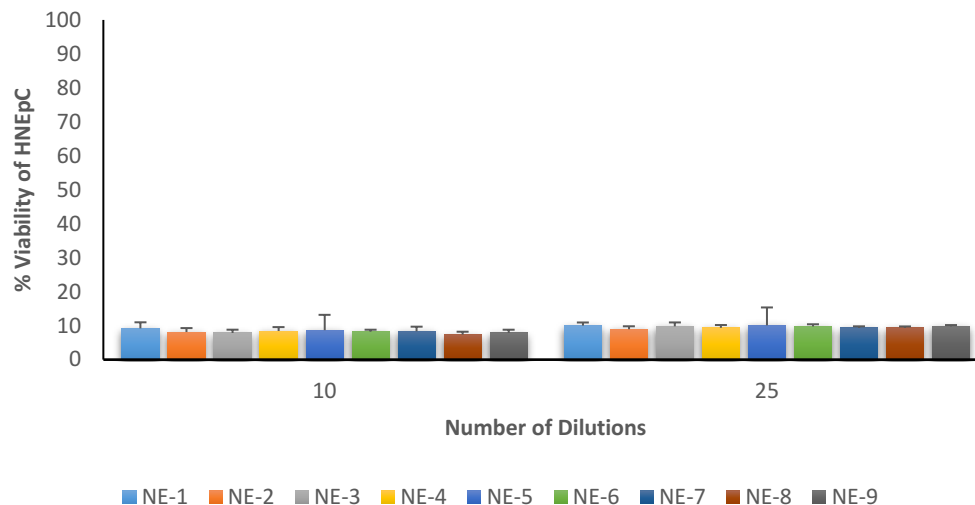


**Fig. 13.** Effect of surfactant Cremophor RH40 on the viability of human nasal epithelial cells after 3 h exposure *in vitro* (mean  $\pm$  S.D., n=6).

### A. Cytotoxicity of Formulations



### B. Cytotoxicity of Formulations

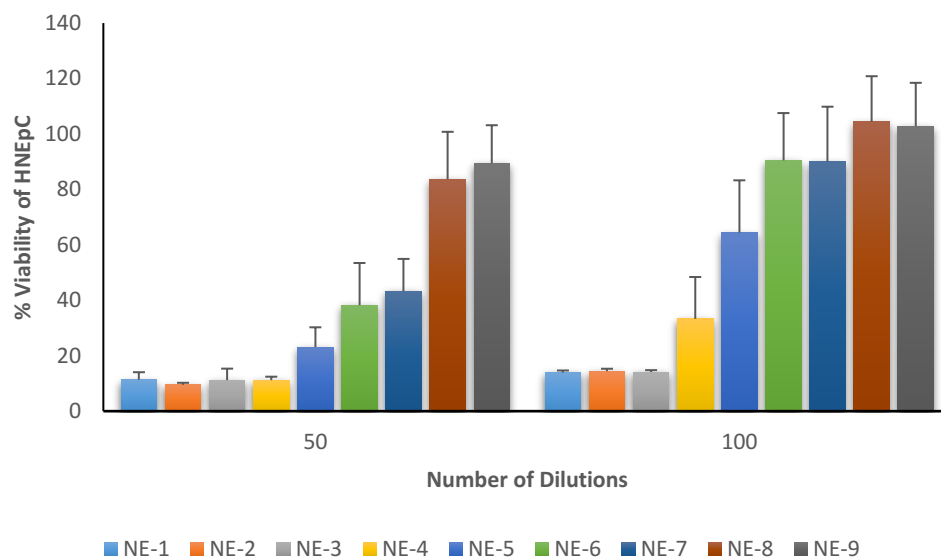


**Fig. 14.** Effect of various nanoemulsions on the viability of HNEpC at: A) 10- and 25-; B) 50- and 100-times dilutions (mean  $\pm$  S.D., n=6).

#### **4.4.5. Preparation of Insulin Complex Loaded Nanoemulsion**

The solubility/dispersibility of Ins-SDC and Ins-SPC complexes in medium chain lipid mixture (Capmul MCM: Captex 8000 = 1:1) was tested and the results are shown in Table 5. Ins-SDC complex was not dispersed at the lowest concentration (0.1%) and this could be due to its salt like properties. Whereas, Ins-SPC complex was dispersed and translucent oil mixture was achieved within the concentration range of 0.1-0.8%. Further studies were carried out on Ins-SPC complex only because Ins-SDC complex was more toxic and less dispersible in lipid mixture than Ins-SPC complex.

The pseudo ternary phase diagram of the 1:1 lipid mixture of capmul MCM:captex 8000 with Cremophor RH40 are depicted in Fig. 15. Nanoemulsion region covers a wide range which indicates that this system can form nanoemulsion with various amount of buffer/water.

The preconcentrate for NE-8 contains 60% of the lipid mixture, and NE-9 contains 50%. More insulin was loaded in NE-8 as compared to NE-9. Therefore, Ins-SPC complex was loaded into the lipid mixture of capmul MCM and captex 8000 (1:1) at the concentration of 0.8%, and then mixed with Cremophor RH40 at 6:4 ratio to form insulin-loaded NE-8 preconcentrate. And nanoemulsions prepared from this preconcentrate were used for further studies.

##### **4.4.5.1. Droplet size of Ins-SPC Loaded NE-8 Nanoemulsion**

Droplet size of Ins-SPC complex loaded NE-8 nanoemulsion was found to in the range of 25 nm to 50 nm when diluted from 5 to 100 times with PBS (Table 6). No

significant difference was observed in droplet size between the blank and the complex-loaded nanoemulsions. Droplet size of blank NE-8 nanoemulsion (5 times dilution) with insulin solubilized in the aqueous phase was determined to be  $32.2 \pm 2.0$  and PDI was determined to be  $0.250 \pm 0.07$ .

#### **4.4.5.2. Leakage of Insulin from the Oil Phase to the Aqueous Phase of the Nanoemulsion**

Leakage of insulin from the complex-loaded oil phase to the aqueous phase of NE-8 nanoemulsion was determined by the membrane centrifugation method with Centriprep 30K tubes (molecular weight cut off: 30,000 Da). Lipid droplets in the nanoemulsion are relatively large, and cannot pass through the membrane, and retains in the donor compartment of the tube, whereas, insulin present in the aqueous phase gets filtered to the receiver compartment as the molecular weight of insulin is 5808 Da which is much lesser than the cut off weight of the membrane. The collected filtrate in the receiver compartment was analyzed for insulin concentration. The insulin concentration in the filtrate was compared to the insulin concentration in the preparation to calculate the percentage leakage, and the results are shown in Table 7. Less than 20% of leakage of insulin from oil phase to aqueous phase was observed for complex-loaded NE-8 nanoemulsion.

**Table 5.** Dispersibility of insulin complexes in the lipid mixture of Capmul MCM and Captex 8000 (1:1).

<b>Complexed Insulin/Lipid Mixture (mg/g)</b>	<b>Ins-SDC Complex</b>	<b>Ins-SPC Complex</b>
10	Not dispersed	Partially dispersed
9	Not dispersed	Partially dispersed
8	Not dispersed	Completely Dispersed
7	Not dispersed	Completely Dispersed
6	Not dispersed	Completely Dispersed
5	Not dispersed	Completely Dispersed
4	Not dispersed	Completely Dispersed
3	Not dispersed	Completely Dispersed
2	Not dispersed	Completely Dispersed
1	Not dispersed	Completely Dispersed

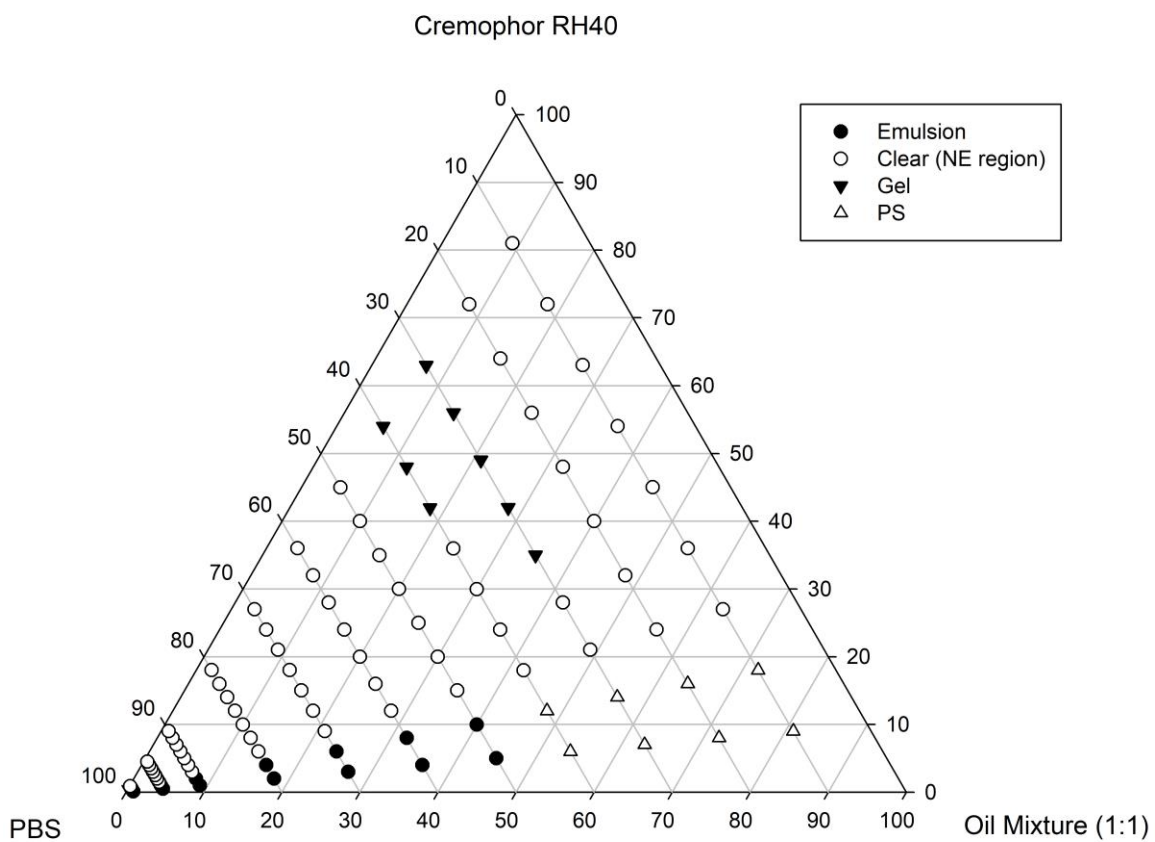


**Fig. 15.** Pseudo-ternary phase diagram.

**Table 6.** Droplet size of NE-8 nanoemulsions with and without Ins-SPC complex loaded in the oil phase (mean  $\pm$  S.D., n=3).

<b>No. of Dilutions with PBS</b>	<b>Blank NE-8 Nanoemulsion</b>	<b>Ins-SPC Complex Loaded NE-8 Nanoemulsion</b>
5	37.9 $\pm$ 5.7	42.8 $\pm$ 7.0
10	36.7 $\pm$ 3.4	34.6 $\pm$ 4.8
25	35.8 $\pm$ 4.3	32.8 $\pm$ 3.8
50	36.1 $\pm$ 1.9	33.4 $\pm$ 3.9
100	36.7 $\pm$ 1.6	34.6 $\pm$ 3.5

**Table 7.** Leakage of insulin from various preparations (mean  $\pm$  S.D., n=3).

---

<b>Name</b>	<b>Leakage (%)</b>
Insulin solution	92.2 $\pm$ 6.4
Ins-SPC complex loaded NE-8	17.4 $\pm$ 2.8

---

#### 4.4.6. Transport of Insulin through Human Nasal Epithelial Cell Monolayer

To predict the absorption of insulin through nasal membrane *in vivo* by the nanoemulsion system, FITC-Ins-SPC complex-loaded NE-8-50X (50 times diluted with transport medium) nanoemulsion along with controls was tested for the transport across human nasal epithelial cell monolayer *in vitro*. NE-8-50X nanoemulsion was selected for transport study as it showed acceptable cytotoxicity (Fig. 14B) and the transported amount of FITC-Insulin was in detectable range.

The transport results are presented in Fig. 16. The transport of insulin by the nanoemulsion system was significantly ( $p < 0.00005$ ) higher than the FITC-Insulin solution, indicating that the nanoemulsion system enhanced the permeability of insulin across HNEpC monolayer. To further investigate whether the enhanced permeation was due to the complexing agent or the nanoemulsion components, FITC-Insulin-SPC complex in buffer and blank NE-8 (without complex) nanoemulsion with FITC-Insulin in its aqueous phase were evaluated for transport. Both the complex suspension and blank NE showed increased transport as compared to the insulin solution. The permeation enhancement by the blank NE-8 with insulin in aqueous phase was significantly ( $p < 0.05$ ) higher than the complex suspension, which indicates that formulation components could have imparted the permeation enhancing effects.

Moreover, the complex-loaded NE-8-50X nanoemulsion presented significantly ( $p < 0.05$ ) higher transport than the blank NE-8-50X nanoemulsion. It can be interpreted from these results that loading insulin inside the oil phase enhances the permeation across

HNEpC monolayer through possible transcellular absorption together with paracellular permeation.

Previously, Rao. et al. and Khatri et. al. have reported that enhanced transport of macromolecules from nanoemulsions could be due to the transport of lipid nano-droplets through epithelial cell monolayer (Khatri and Shao, 2017b; Rao et al., 2008a). Therefore, to evaluate the transport of lipid droplets, the droplet size was measured in the donor and receiver side at the end of transport study to confirm the transport of lipid nano-droplets through human nasal epithelial cell monolayer (Table 8). Droplet size in the donor or receiver chamber was not detected in case of FITC-Insulin solution. For the complex suspension, droplet size of about 1000 nm was observed in the receiver chamber which indicates phosphatidylcholine present in complex may have interacted and fused through the cells or through the tight junctions. Complex loaded nanoemulsion NE-8-50X showed higher droplet size in the receiver chamber than the donor chamber which could have been due to the presence of phosphatidylcholine. Blank nanoemulsion also showed slightly higher droplet size indicating that the droplets when passing through cell membrane may have interacted with cell components and may have transported to the receiver side.

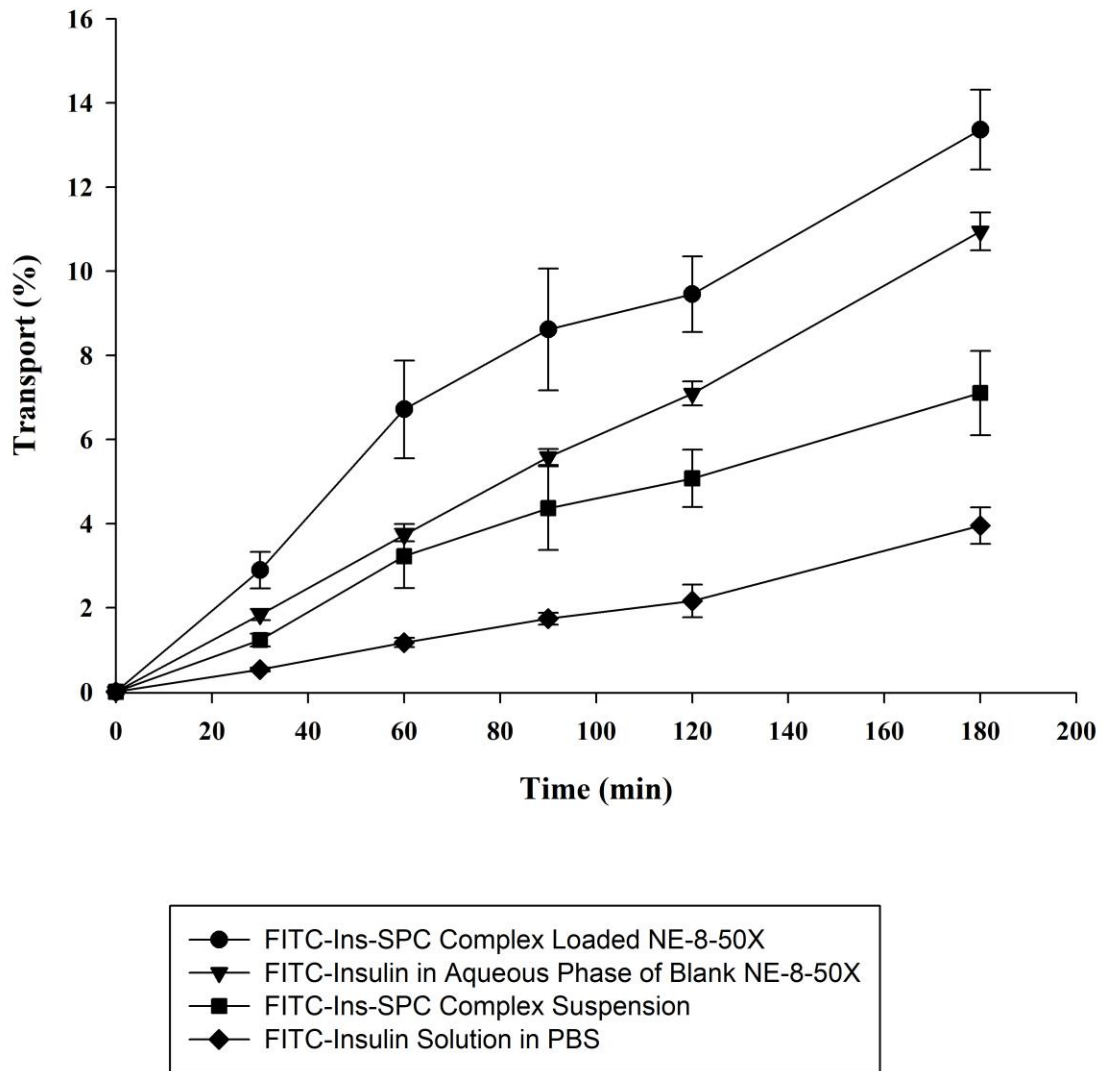


**Fig. 16.** Permeability of complex loaded nanoemulsion, blank nanoemulsion with insulin in aqueous phase, complex suspension and insulin solution through HNEpC monolayer, (mean  $\pm$  S.D., n=6).

**Table 8.** Droplet size in the donor and receiver side at the end of the transport study through HNEpC monolayer (mean  $\pm$  SD, n  $\geq$  5).

<b>Formulation</b>	<b>Droplet Size (nm)</b>	
	<b>Donor Side</b>	<b>Receiver side</b>
FITC-Insulin solution	ND	ND
Complex suspension	4057.5 $\pm$ 2190.7	1023.9 $\pm$ 168.5
FITC-Ins-SPC complex-loaded NE-8 nanoemulsion	36.6 $\pm$ 2.6	114.4 $\pm$ 39.8
Blank NE-8 nanoemulsion with FITC-Insulin in aqueous phase	37.8 $\pm$ 3.6	51.2 $\pm$ 7.6

ND: Not detected

#### **4.4.7. Effect of the NE-8 Nanoemulsion on the Integrity of the HNEpC Monolayer**

To evaluate the impact of the formulation on the integrity of the human nasal epithelial cell monolayer, permeability of the paracellular marker and transcellular marker in presence of NE-8-50X nanoemulsion and other controls was studied.

Propranolol undergoes passive transcellular transport as it is a lipophilic (Log P 2.53) molecule with molecular weight of 259.3 g/mol. Mannitol transports through passive paracellular transport as it is a highly hydrophilic molecule (Log P -2.5) with low molecular weight of 182.2 g/mol (Kaushal et al., 2006). Therefore, propranolol and mannitol have been used as the transcellular and paracellular marker, respectively, to determine the integrity of the cell monolayers.

As shown in Fig. 17, there was no significant difference in the transport amongst Ins-SPC complex-loaded NE-8-50X nanoemulsion and blank NE-8-50X with insulin in aqueous phase and insulin solution. These results indicate that the monolayer's integrity was maintained throughout the transport study. The cumulative transport of propranolol at 3 h decreased significantly in presence of Ins-SPC complex suspension ( $p < 0.005$ ) compared to the other three cases. It could be because of SPC which may have hindered the transport of propranolol by creating a viscous layer on top of the monolayer.

The transport of the paracellular marker mannitol is depicted in Fig. 18. Results showed that mannitol's permeability after 3 h of cumulative transport didn't change significantly for NE-8 formulation and blank NE. However, mannitol's transport significantly decreased ( $p < 0.05$ ) in presence of complex suspension. Again, this could be

due to viscous nature of SPC. Results indicate that cell monolayer was intact throughout the study and the enhanced permeability was not due to cell damage.

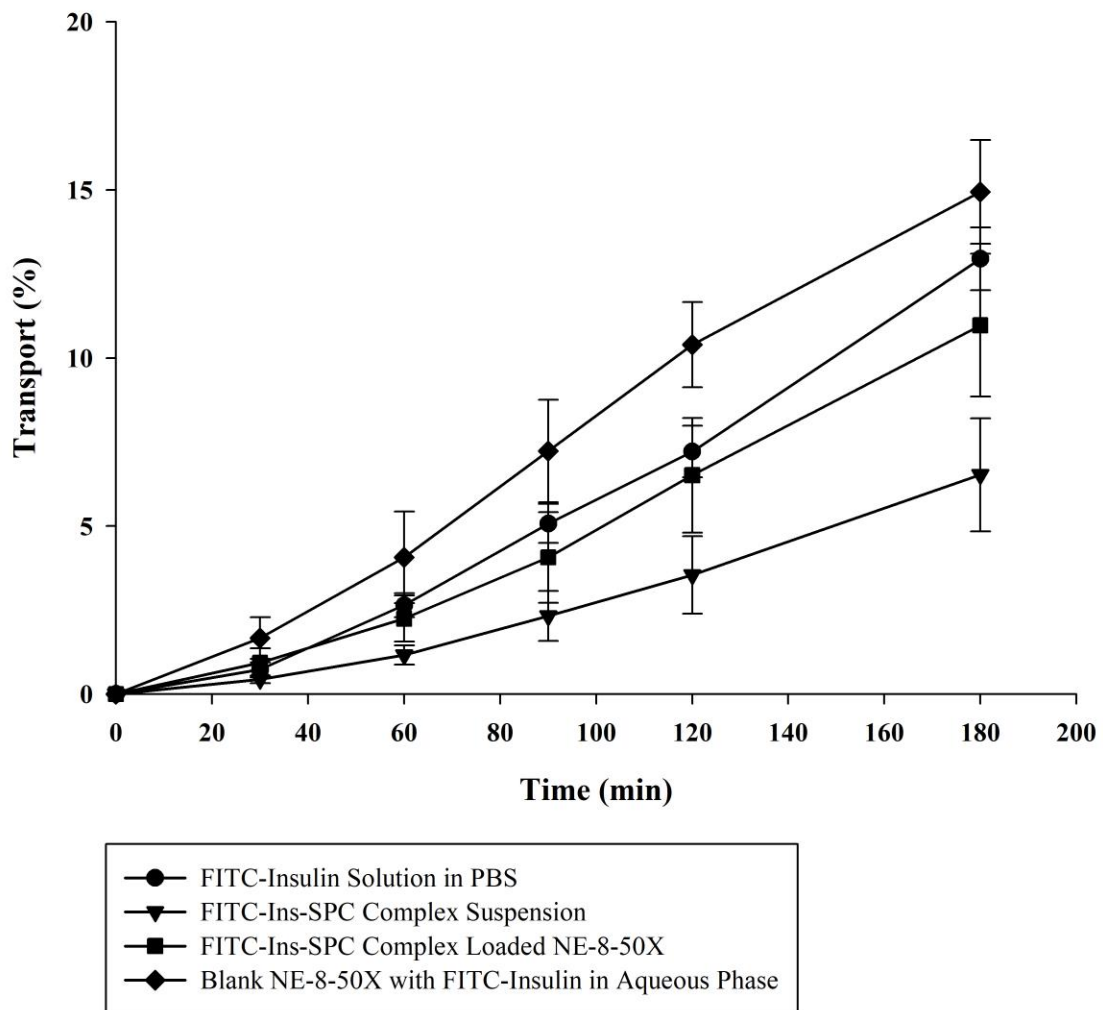
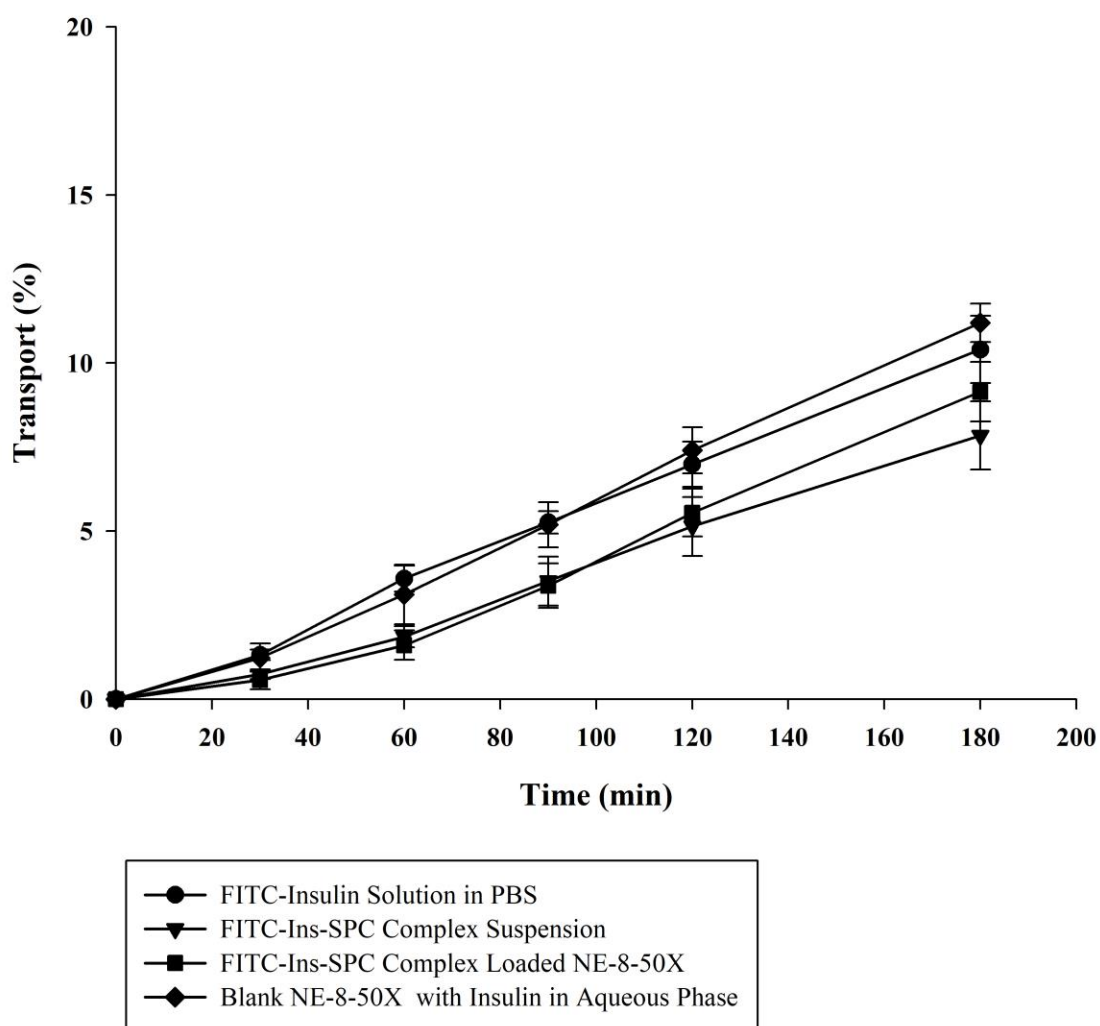


Fig. 17. Permeability of Propranolol through HNEpC monolayer (mean  $\pm$  S.D., n=6).



**Fig. 18.** Permeability of Mannitol through HNEpC monolayer (mean  $\pm$  S.D., n=6).

#### **4.5. Conclusion**

Lipophilic complexes of insulin and insulin loaded nanoemulsions were successfully developed and characterized. Ins-SPC complex loaded nanoemulsion with acceptable toxicity enhanced the permeation of insulin by three times as compared to insulin solution.

## CHAPTER 5. *IN-VIVO* ANIMAL STUDY

### 5.1. Introduction

Various animal models have been used for intranasal delivery of insulin. From small animals such as guinea pigs, hamsters, mice and rats to big animals such as rabbits, dogs, monkeys and sheep. Although big animals are preferred over small animals for their large nasal cavity which can allow more delivery volume, they are expensive to use. Rats are often used as the animal model for *in vivo* study as it is easy to handle, inexpensive and provides sufficient volume of blood for pharmacokinetic studies (Ehrhardt and Kim, 2008; Gizurarson, 1990). Moreover, rat and human nasal cavity have similar anatomical features, nasal cavity is divided into two main air passages by the nasal septum (Chamanza and Wright, 2015).

Insulin deficiency in diabetic rats causes extreme changes in metabolism, a reduction in liver protein synthesis, dehydration, decreased activity of the sympathetic nervous system, and osmotic diuresis (Anwana and Garland, 1991; Yoshida et al., 1985). Also, streptozotocin-induced diabetic rats show a different response profile to environmental stress factors (Bellush and Henley, 1990). Linn et. al. studied the intranasal absorption of insulin in diabetic and non-diabetic rats and observed increased variability of blood glucose levels in the diabetic rats as compared to healthy rats (Simon et al., 2005). Therefore, in order to minimize the variability in blood glucose levels due to physiological changes in diabetic rats, we have selected healthy rat as an animal model for our study.

### **Specific objectives of the study:**

- To determine whether insulin loaded in the oil phase of nanoemulsion can enhance intranasal absorption of insulin
- To evaluate the toxicity effect of formulation components on nasal membrane

### **5.2. Materials**

Human insulin (27.5 IU/mg) was purchased from Sigma-Aldrich, Co. (St. Louis, MO, USA). L- $\alpha$ -phosphatidylcholine (Soy 95%) was purchased from Avanti Polar Lipids, Inc. (Alabama, USA). AimStrip® Plus Glucose meter was purchased from ERMAINE LABORATORIES, INC (San-Antonio, TX, USA). Human Insulin ELISA Kit was purchased from Crystal Chem (Elk Grove Village, IL, USA). Lithium heparin tubes were purchased from SARSTEDT AG & Co. (Nümbrecht, Germany). Stainless steel disposable scalpels were purchased from Intergra York PA, Inc (PA, USA). Lidocaine Hydrochloride Jelly USP, 2% was purchased from Akron, Lake Forest (IL, USA). Animal feeding needles were purchased from Cadence Science, Inc. (Plainfield Pike Cranston, RI, USA). Isoflurane, USP was purchased from HENRY SCHEIN (Dublin, OH, USA). Sterile gauze sponges were purchased from Dukal Corporation (Ronkonkoma, NY, USA).

### **5.3. Methods**

#### **5.3.1. Animal Study Procedure**

Male Sprague Dawley rats weighing 280-400 gram were used for this study. The rats were randomly divided into six groups with six rats in each group (Table 9). The rats were fasted for 12 h prior to experiment with water ad libitum. The rats were anesthetized by 3% isoflurane. Once anesthetized, the rats were taken out of the isoflurane chamber and were kept in a supine position on a soft-temp reusable veterinary heating pad with nose cone attached to deliver 2% isoflurane for maintenance of unconscious effect.

The rats were anesthetized for 30 min before dosing to stabilize the blood glucose level and the blood glucose was measured every 5-10 min. Effect of anesthesia on blood glucose level was evaluated by monitoring anesthetized rat's blood glucose level for 4 h without administering any formulation. One ml of 20% glucose was given by intraperitoneal injection if the blood glucose level dropped below 30 mg/dL while performing the study (Mcnay et al., 2013).

For intranasal delivery, 3.6 IU/kg of human insulin in about 50  $\mu$ l of various formulations was administered to the nasal cavity via the right nostril by a micro syringe connected to a polyethylene tubing which was inserted about 0.6 cm into the nostril. For subcutaneous delivery, 1 IU/kg human insulin in about 500  $\mu$ l buffer (PBS, pH 7.4) was given at loose skin over the back muscle. Blood samples (100 – 200  $\mu$ l, depending on rat's body weight) were collected by tail tipping into heparin coated microcentrifuge tubes immediately before dosing and at 5, 15, 30, 45, 60, 90, 120, 180 & 240 min after

the administration. The blood glucose level was measured using AimStrip® Plus Blood Glucose Meter each time the blood was collected and noted. The blood samples were centrifuged at 9000 rcf for 10 min at 4° C and the plasma was collected. The plasma samples were stored at -20° C until further analysis. Plasma concentration of insulin was determined by ELISA (Enzyme-linked immunosorbent assay). Standard non-compartmental analysis was performed for determination of the pharmacokinetic parameters

All the rats were euthanized by carbon dioxide (CO<sub>2</sub>) right after the experiment was completed. After euthanasia, the head of the rat was collected and stored in 10% formalin solution for the histology study on the nasal membrane.

### **5.3.2. ELISA Assay**

The insulin ELISA kit used for sample analysis was specific to human insulin and didn't react with rat's inherent insulin present in plasma. ELISA kit used was designed on a principle of sandwich assay by utilizing a specific antibody immobilized onto the microplate wells and an antibody labeled with HRP enzyme.

#### **ELISA Assay procedure**

All reagents were brought to room temperature for at least 30 min prior to running the assay. In each well of a 96-well microplate, 100 µl of working HRP labeled antibody followed by 25 µl of plasma sample or kit's standard was added and mixed well by repeated pipetting. Microplate was sealed with sealer and incubated at 37° C for 2 h. The contents were aspirated from the wells after incubation and the wells were washed three

times using 300  $\mu$ l wash buffer. After each wash, any remaining solution in the well was removed by inverting and tapping the plate firmly on a clean paper towel. After washing, 100  $\mu$ l of the substrate solution was added to each well and incubated in dark for 15 min at room temperature. Reaction was stopped by adding 100  $\mu$ l of the stop solution.

Absorbance ( $A_{450}$ ) was measured by a plate reader. A standard curve with the kit's standards and the concentration of insulin in plasma samples was calculated according to standard curve.

**Table 9.** Animal groups for the *in-vivo* study.

<b>Animal Group #</b>	<b>Treatment</b>
1	Buffer (PBS) without insulin, 50 µl, intranasal
2	Insulin solution (PBS), 3.6 IU/kg, 50 µl, intranasal
3	Ins-SPC complex loaded in the oil phase of NE-8-5X, 3.6 IU/kg, 50 µl, intranasal
4	Ins-SPC complex suspension, 3.6 IU/kg, 50 µl, intranasal
5	Blank NE-8-5X with insulin solubilized in aqueous phase, 3.6 IU/kg, 50 µl, intranasal
6	Insulin buffer solution by subcutaneous route, 1 IU/kg, 500 µl, subcutaneous

### **5.3.3. Histological Study**

Histological examination was carried out to determine any toxic effect of the formulations on nasal membrane by the examination for any signs of epithelial disorganization, cilia disappearance and slight dysplastic changes.

Three animals from each group of nasal administration were evaluated for histology study. The nasal cavity tissue was collected, decalcified and was dehydrated with 100%, 95%, 80%, 70% alcohol. The resulting blocks were embedded in paraffin and thin cross-sections of samples were prepared on a microtome and stained with hematoxylin-eosin for light microscopic observation (Piao et al., 2010).

## **5.4. Data Analysis**

For data analysis, all the values were expressed as mean  $\pm$  S.D. or SEM. Statistical analysis was performed by student's t-test. A value of  $p < 0.05$  was considered to be statistically significant.

## **5.5. Results**

### **5.5.1. *In-vivo* Absorption Study**

For *in-vivo* absorption study, insulin dose (3.6 IU/kg) was decided based on previously published reports and expected pharmacological activity. In order to deliver 3.6 IU/kg of insulin, NE-8 concentrate was diluted 5 times with PBS (NE-8-5X).

Some of the rats had died during the study due to lack of animal study experience and device/technical issues related to anesthesia system. Hence, we had used 3 rats/group for complex suspension and insulin solution groups and 6 rats/group for subcutaneous injection, Ins-SPC complex loaded NE-8-5X and blank NE-8-5X with insulin in aqueous phase.

From the study on effect of anesthesia on blood glucose level, it was observed that glucose level remained between 95% -100% during the entire study time (data not shown). This confirmed the absence of anesthesia effect on glucose level.

Hypoglycemic effect after dosing of various formulations is depicted in Fig. 19, and the pharmacodynamic parameters are presented in Table 10. Subcutaneous delivery of 1 IU/kg insulin reduced maximum blood glucose levels by approximately 52%. Area above the curve for SC delivery was used as reference for calculating the relative pharmacological availability (PA) of nasally administered insulin. PA was calculated by following equation:

$$\% PA = \frac{AAC_{f(0-240min)}/Dose_{in}}{AAC_{sc(0-240min)}/Dose_{sc}} \times 100 \quad \text{Eq. 4}$$

where,  $AAC_f$  is area above the curve of glucose reduction-time curve of formulation or buffer group;  $AAC_{sc}$  is area above the curve of glucose reduction-time curve of subcutaneous injection group,  $Dose_{in}$  is intranasal delivery dose and  $Dose_{sc}$  is subcutaneous delivery dose.

Insulin solution and buffer (PBS, pH 7.4) without drug showed similar response of glucose level with the maximum glucose reduction of approximate 20%. The PA of

buffer and insulin solution group was observed to be  $11.8 \pm 1.4$  and  $13.1 \pm 2.3$ , respectively. Ins-SPC complex suspension (prepared in buffer PBS), insulin in aqueous phase of blank NE-8-5X and Ins-SPC complex loaded NE-8 showed up to 40%, 60% and 70% maximum glucose reduction with mean relative PA of  $23.5 \pm 2.9$ ,  $30.1 \pm 4.1$  and  $36.2 \pm 3.6$ , respectively.

The plasma insulin concentration vs time profile and pharmacokinetic parameters are shown in Fig. 20 and Table 10, respectively. Subcutaneous administration of insulin solution presented  $C_{\max}$  of  $77.6 \pm 9.2 \mu\text{U/ml}$  and  $AUC_{0-240\text{min}}$  of  $77.1 \pm 12.6 (\mu\text{U} * \text{h/ml})$ . This AUC value of subcutaneous delivery was used as a reference for the calculation of the relative bioavailability (BA) of the intranasally administered insulin. BA was calculated by following equation:

$$\% BA = \frac{AUC_f(0-240\text{min})/Dose_{in}}{AUC_{sc}(0-240\text{min})/Dose_{sc}} \times 100 \quad \text{Eq. 5}$$

where,  $AUC_f$  is area under the insulin-time curve of formulation or buffer group;  $AUC_{sc}$  is area under the curve of insulin-time curve of subcutaneous injection group,  $Dose_{in}$  is intranasal delivery dose and  $Dose_{sc}$  is subcutaneous delivery dose.

The intranasal administration of insulin solution showed minimal absorption (Fig. 20) with  $C_{\max}$  of  $5.8 \pm 1.9 \mu\text{U/ml}$  and the bioavailability of  $5.5 \pm 1.4 \%$ . The administration of Ins-SPC complex suspension resulted in small elevation of plasma insulin concentration with  $C_{\max}$  of  $12.9 \pm 6.8 \mu\text{U/ml}$ , and bioavailability of  $6.8 \pm 2.0 \%$ . These results indicate that complexing agent SPC had little permeation enhancing effects in delivering insulin nasally.

Significantly higher absorption was observed when insulin solubilized in aqueous phase of blank NE-8-5X and Ins-SPC complex loaded NE-8-5X formulations were administered. Blank NE-8-5X with insulin in aqueous phase showed  $C_{\max}$  of  $199.7 \pm 38.6$   $\mu\text{U/ml}$  ( $p < 0.01$ ) with bioavailability of  $43.8 \pm 7.1$  % ( $p < 0.01$ ) compared to the free solution form and complex suspension with  $T_{\max}$  of about 11 min. However, when insulin was loaded in the oil phase of nanoemulsion system (NE-8-5X), maximum plasma concentration was observed to be  $255.9 \pm 35.9$   $\mu\text{U/ml}$  ( $p < 0.001$ ) and bioavailability was determined to be  $68.8 \pm 8.7$  % ( $p < 0.001$ ) compared to the free solution form and complex suspension with  $T_{\max}$  of 15 min.

These results were in correlation with *in vitro* transport results which indicated that the enhanced absorption of insulin could be due to permeation enhancing properties of formulation component capmul MCM. Although capmul MCM at concentrations higher than 1% showed toxic effects on cells, we hypothesize that it may not be as toxic as it is on cell monolayer for *in vivo* delivery because of the membrane thickness and fast membrane recovery. Kim et. al. performed the histological examination of rat's nasal membrane 6 h after an intranasal delivery of microemulsion containing 15% of capmul MCM and observed negligible toxicity to the nasal epithelium (Cho et al., 2012). Our *in vivo* study formulation contains about 6% of capmul MCM which is much lower than the reported non-toxic concentration. To further confirm and evaluate the toxicity effect of our formulation on nasal membrane, histological examination was carried out.

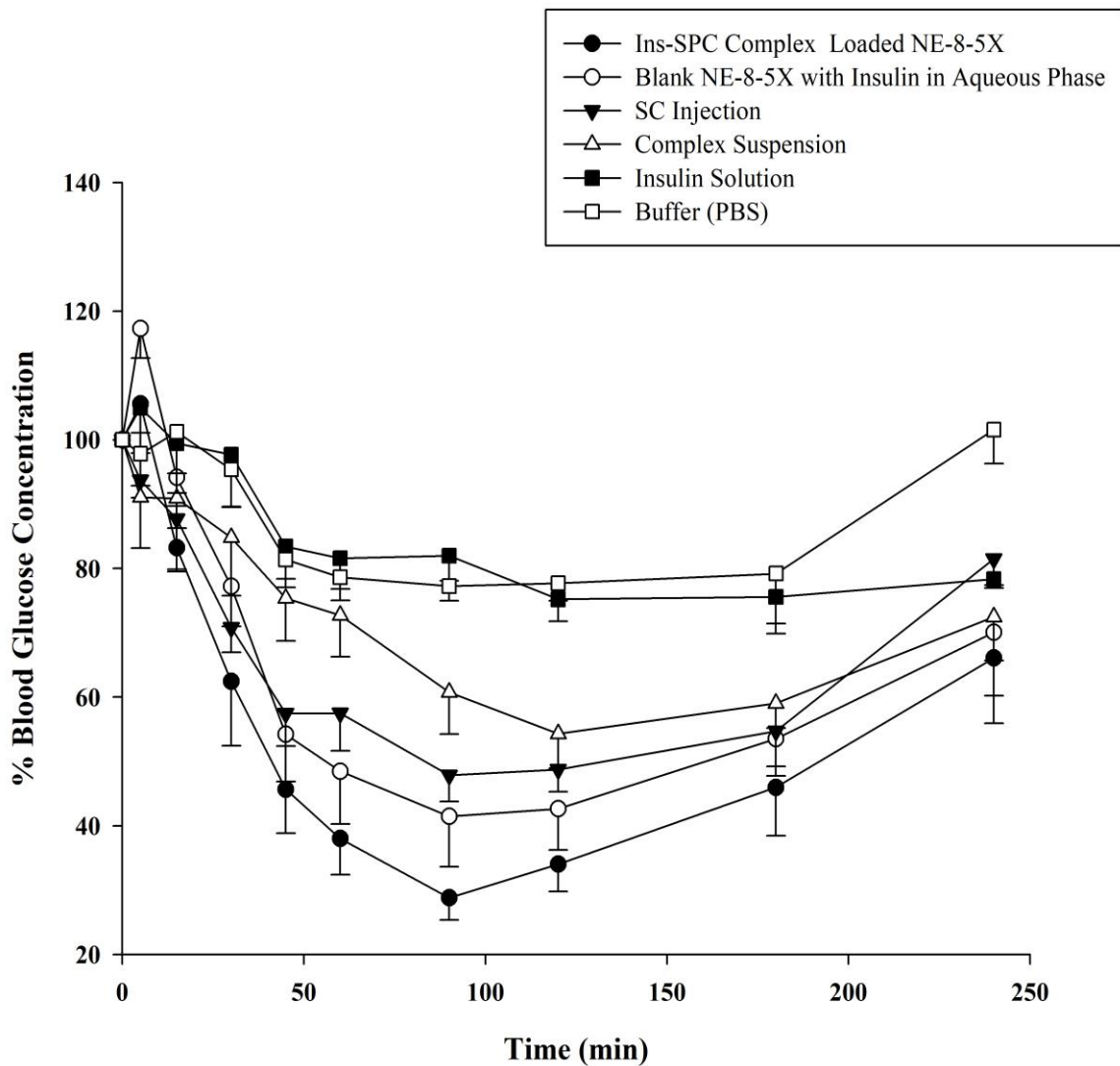


**Fig. 19.** Blood glucose reduction in healthy rats following 1 IU/kg subcutaneous dose and 3.6 IU/kg nasal delivery dose (mean  $\pm$  SEM, n = 3-6).

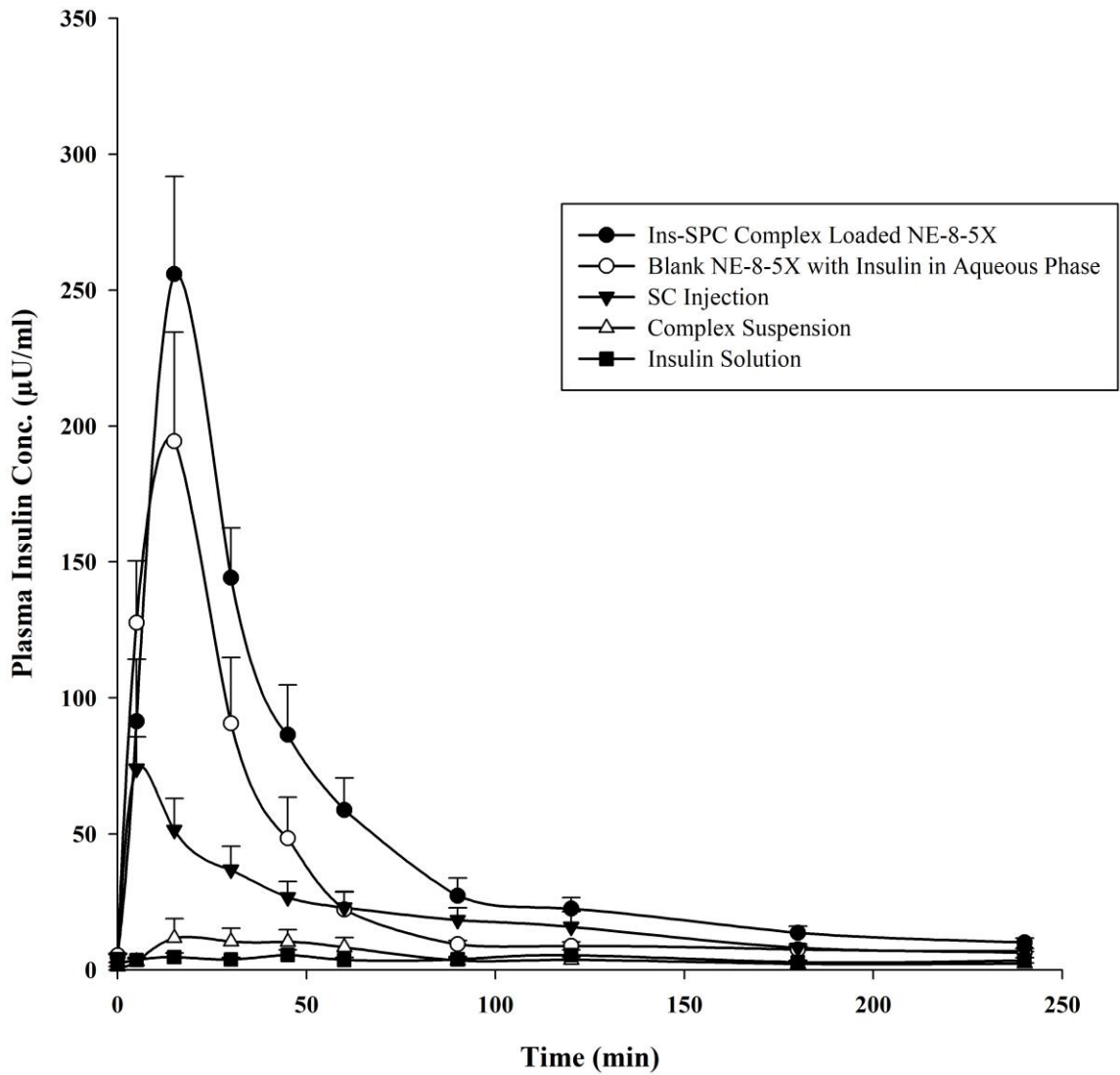


**Fig. 20.** Plasma insulin conc. vs time profiles following nasal administration of 3.6 IU/kg and 1 IU/kg subcutaneous administration in healthy rats (mean  $\pm$  SEM, n = 3-6).

**Table 10.** Pharmacokinetic and pharmacodynamic parameters (mean  $\pm$  SEM, n = 3-6).

Group Name	NE-8 Formulation (n=6)	Insulin in Aq. Phase of NE-8 (n=6)	Complex Suspension (n=3)	Insulin Solution (n=3)	Buffer PBS (n=5)	Insulin Solution S.C. (n=6)
$C_{max}$ ( $\mu$ U/ml)	<sup>c</sup> 255.9 $\pm$ 35.9***	<sup>b</sup> 199.7 $\pm$ 38.6**	12.9 $\pm$ 6.8	5.8 $\pm$ 1.9	-	77.6 $\pm$ 9.2
$T_{max}$ (min)	15.0	11.7 $\pm$ 2.1	35.0 $\pm$ 10.2	20.0 $\pm$ 5.0	-	6.8 $\pm$ 1.5
AAC <sub>0-240 min</sub> (% Glu. Reduction* <sub>h</sub> )	<sup>a</sup> 203.6 $\pm$ 20.2***	169.4 $\pm$ 23.3**	132.6 $\pm$ 16.5	73.5 $\pm$ 12.8	66.6 $\pm$ 7.7	156.5 $\pm$ 11.0
AUC <sub>0-240 min</sub> ( $\mu$ U * h/ml)	<sup>c</sup> 190.9 $\pm$ 24.0***	<sup>b</sup> 121.7 $\pm$ 19.6**	18.9 $\pm$ 5.6	15.5 $\pm$ 3.8	-	77.1 $\pm$ 12.6
Relative PA (%)	<sup>a</sup> 36.2 $\pm$ 3.6***	30.1 $\pm$ 4.1**	23.5 $\pm$ 2.9	13.1 $\pm$ 2.3	11.8 $\pm$ 1.4	100
Relative BA (%)	<sup>c</sup> 68.8 $\pm$ 8.7***	<sup>b</sup> 43.8 $\pm$ 7.1**	6.8 $\pm$ 2.0	5.5 $\pm$ 1.4	-	100

\* $p < 0.05$ , \*\* $p < 0.01$ , \*\*\* $p < 0.001$ , significant difference compared with the insulin solution group. <sup>a</sup> $p < 0.05$ , <sup>b</sup> $p < 0.01$ , <sup>c</sup> $p < 0.001$ , significant difference compared with the complex suspension group.

Nasal administration dose = 3.6 IU/kg, subcutaneous administration dose = 1IU/kg

$C_{max}$ : maximum insulin concentration;  $T_{max}$ : time to reach  $C_{max}$ ; AAC: area above the glucose-time curve; AUC: area under the insulin-time curve; PA: relative pharmacological availability compared with s.c; BA: relative bioavailability compared with s.c.

### **5.5.2. Histology Study**

Toxicity of the various formulations on the nasal epithelium was evaluated by histological staining. No apparent damage to the mucosal membrane was observed in case of insulin complex-loaded nanoemulsion (NE-8-5X) as compared to insulin solution. The results are presented in Fig. 21.

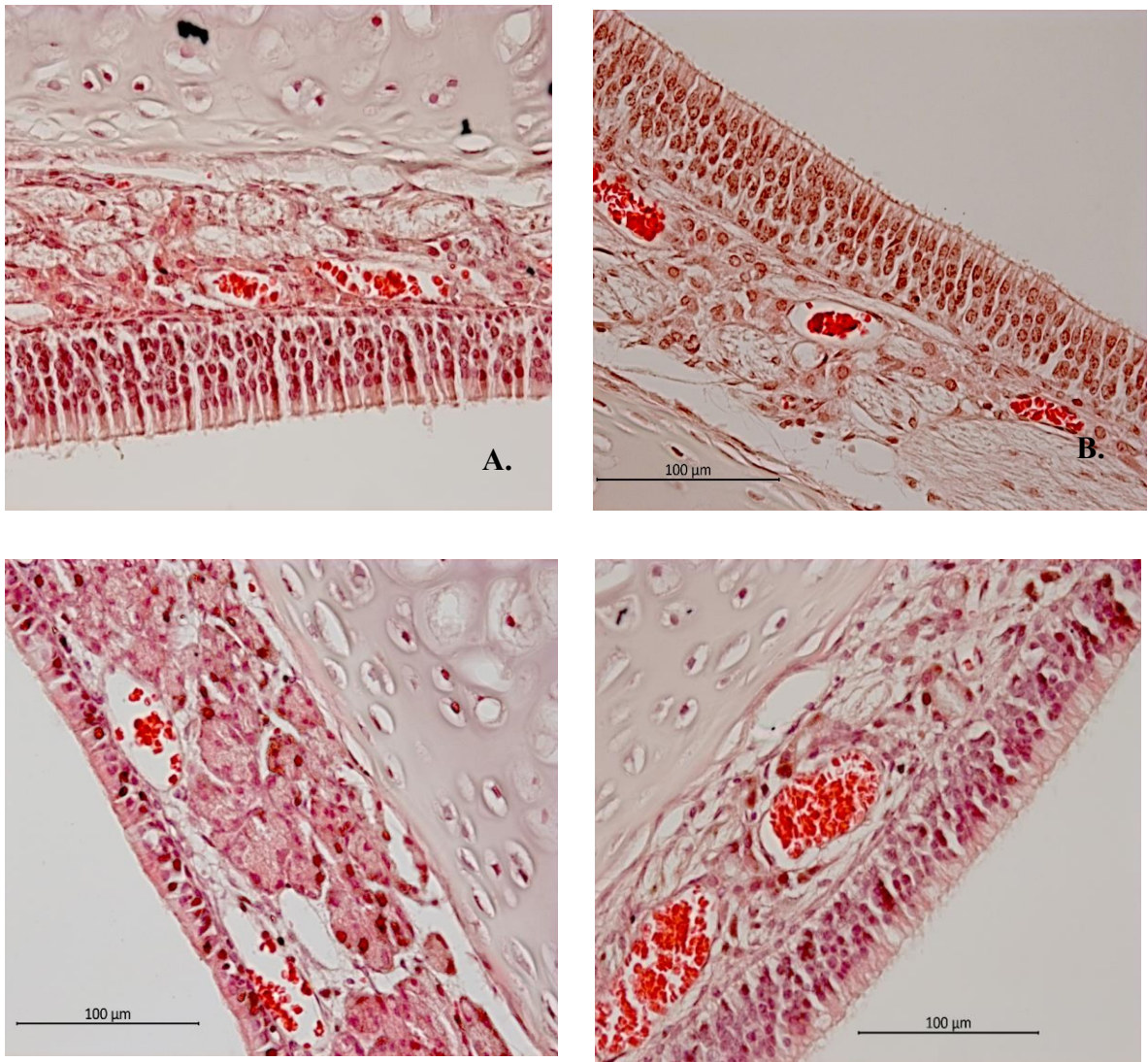


**Fig. 21.** Photomicrographs of nasal mucosal membrane (vertical sections cut through the respiratory mucosa of nasal cavity) following nasal administration of A.) Insulin solution in PBS and B.) Ins-SPC complex loaded nanoemulsion (NE-8-5X) C.) Blank nanoemulsion with insulin in aqueous phase and D.) Ins-SPC complex suspension for 4 h. Tissues were fixed in 10% neutral buffered formalin, decalcified, and stained with H & E. The microscopic observation was carried out using a 40X objective lens.

## **5.6. Conclusion**

Ins-SPC complex loaded nanoemulsion has promising potential to deliver insulin by nasal route.

## CHAPTER 6: FUTURE STUDIES

Following studies will be conducted in future:

1. Evaluation of different doses to measure insulin concentration and blood glucose reduction in healthy and diabetic rats for dose response curve using Ins-SPC complex loaded nanoemulsion system.
2. Chronic toxicity effect of developed formulation on rat's nasal mucosa after multiple dose administration will be investigated by histological examination.
3. Evaluation of nasal absorption of insulin through nanoemulsion system where insulin is loaded into the oil phase as well as in the aqueous phase.
4. Use of insulin analogues with developed formulation to determine absorption profile *in-vivo*.
5. Exploration of developed formulation for treatment of Alzheimer's disease.

## REFERENCES

- AboutFotouh, K., Allam, A.A., El-Badry, M., El-Sayed, A.M., 2018. Role of self-emulsifying drug delivery systems in optimizing the oral delivery of hydrophilic macromolecules and reducing interindividual variability. *Colloids Surfaces B Biointerfaces* 167, 82–92. <https://doi.org/10.1016/j.colsurfb.2018.03.034>
- Adjei, A., Sundberg, D., Miller, J., Chun, A., 1992. Bioavailability of leuprolide acetate following nasal and inhalation delivery to rats and healthy humans. *Pharm. Res.* 9, 244–249.
- Anderberg, E.K., Lindmark, T., Artursson, P., 1993. Sodium Caprate Elicits Dilatations in Human Intestinal Tight Junctions and Enhances Drug Absorption by the Paracellular Route. *Pharm. Res.* 10, 857–864. <https://doi.org/10.1023/A:1018909210879>
- Anwana, A.B., Garland, H.O., 1991. Intracellular dehydration in the rat made diabetic with streptozotocin: effects of infusion. *J. Endocrinol.* 128, 333–7.
- Arora, P., Sharma, S., Garg, S., 2002. Permeability issues in nasal drug delivery. *Drug Discov. Today* 7, 967–975.
- Aungst, B.J., Hussain, M.A., 1992. Sustained Propranolol Delivery and Increased Oral Bioavailability in Dogs Given a Propranolol Laurate Salt. *Pharm. Res.* 09, 1507–1509. <https://doi.org/10.1023/A:1015831517800>
- Aungst, B.J., Rogers, N.J., 1988. Site dependence of absorption-promoting actions of laureth-9, Na salicylate, Na<sub>2</sub>EDTA, and aprotinin on rectal, nasal, and buccal insulin delivery. *Pharm. Res.* 5, 305–308.

- Banks, P.R., Paquette, D.M., 1995. Comparison of Three Common Amine Reactive Fluorescent Probes Used for Conjugation to Biomolecules by Capillary Zone Electrophoresis. *Bioconjugate Chem* 6, 447–458.
- Behl, C.R., Pimplaskar, H.K., Sileno, A.P., Xia, W.J., Gries, W.J., Demeireles, J.C., Romeo, V.D., 1998. Optimization of systemic nasal drug delivery with pharmaceutical excipients. *Adv. Drug Deliv. Rev.* 29, 117–133.
- Bellush, L.L., Henley, W.N., 1990. Altered responses to environmental stress in streptozotocin-diabetic rats. *Physiol. Behav.* 47, 231–238.  
[https://doi.org/10.1016/0031-9384\(90\)90136-R](https://doi.org/10.1016/0031-9384(90)90136-R)
- Bromer, W.W., Sheehan, S.K., Berns, A.W., Arquilla, E.R., 1967. Preparation and Properties of Fluoresceinthiocarbamyl Insulins. *Biochemistry* 6, 2378–2388.  
<https://doi.org/10.1021/bi00860a013>
- Brooking, J., Davis, S.S., Illum, L., 2001. Transport of nanoparticles across the rat nasal mucosa. *J. Drug Target.* 9, 267–279.
- Bruno, B.J., Miller, G.D., Lim, C.S., 2013. Basics and recent advances in peptide and protein drug delivery. *Ther. Deliv.* 4, 1443–1467.
- Callens, C., Pringels, E., Remon, J.P., 2003. Influence of multiple nasal administrations of bioadhesive powders on the insulin bioavailability. *Int. J. Pharm.* 250, 415–422.
- Chamanza, R., Wright, J.A., 2015. A Review of the Comparative Anatomy, Histology, Physiology and Pathology of the Nasal Cavity of Rats, Mice, Dogs and Non-human Primates. Relevance to Inhalation Toxicology and Human Health Risk Assessment. *J. Comp. Pathol.* 153, 287–314. <https://doi.org/10.1016/J.JCPA.2015.08.009>

- Cho, H.-J., Ku, W.-S., Termsarasab, U., Yoon, I., Chung, C.-W., Moon, H.T., Kim, D.-D., 2012. Development of udenafil-loaded microemulsions for intranasal delivery: In vitro and in vivo evaluations. *Int. J. Pharm.* 423, 153–160.  
<https://doi.org/10.1016/J.IJPHARM.2011.12.028>
- Cho, H.-J., Termsarasab, U., Kim, J.-S., Kim, D.-D., 2010. In vitro Nasal Cell Culture Systems for Drug Transport Studies. *J. Pharm. Investig.* 40, 321–332.
- Corbo, D.C., Liu, J., Chienx, Y.W., 1990. Characterization of the barrier properties of mucosal membranes. *J. Pharm. Sci.* 79, 202–206.
- Cui, F., Shi, K., Zhang, L., Tao, A., Kawashima, Y., 2006. Biodegradable nanoparticles loaded with insulin–phospholipid complex for oral delivery: Preparation, in vitro characterization and in vivo evaluation. *J. Control. Release* 114, 242–250.  
<https://doi.org/10.1016/J.JCONREL.2006.05.013>
- Dai, W.-G., Dong, L.C., 2007. Characterization of physiochemical and biological properties of an insulin/lauryl sulfate complex formed by hydrophobic ion pairing. *Int. J. Pharm.* 336, 58–66. <https://doi.org/10.1016/J.IJPHARM.2006.11.035>
- Davis, S.S., Illum, L., 2003. Absorption enhancers for nasal drug delivery. *Clin. Pharmacokinet.* 42, 1107–1128.
- Dondeti, P., 1991. Development of a new non-surgical perfusion technique to evaluate nasal drug delivery.
- Donovan, M.D., Huang, Y., 1998. Large molecule and particulate uptake in the nasal cavity: the effect of size on nasal absorption. *Adv. Drug Deliv. Rev.* 29, 147–155.
- Edman, P., Björk, E., Ryden, L., 1992. Microspheres as a nasal delivery system for

- peptide drugs. *J. Control. Release* 21, 165–172.
- Ehrhardt, C., Kim, K., 2008. Drug absorption studies : in situ, in vitro and in silico models. Springer.
- Gad, S.C., 2008. Nasal delivery of peptide and nonpeptide drugs : Pharmaceutical Manufacturing Handbook: production and processes. John Wiley & sons.
- Gad, S.C., Wiley InterScience (Online service), 2008. Pharmaceutical manufacturing handbook : production and processes. Wiley-Interscience.
- Gaudana, R., Khurana, V., Parenky, A., Mitra, A.K., 2011. Encapsulation of Protein-Polysaccharide HIP Complex in Polymeric Nanoparticles. *J. Drug Deliv.* 2011, 458128. <https://doi.org/10.1155/2011/458128>
- Gizurarson, S., 1990. Animal models for intranasal drug delivery studies. A review article. *Acta Pharm. Nord.* 2, 105–122.
- Goddeeris, C., Cuppo, F., Reynaers, H., Bouwman, W.G., Van den Mooter, G., 2006. Light scattering measurements on microemulsions: Estimation of droplet sizes. *Int. J. Pharm.* 312, 187–195.
- Gök, E., Olgaz, S., 2004. Binding of fluorescein isothiocyanate to insulin: A fluorimetric labeling study. *J. Fluoresc.* 14, 203–206.  
<https://doi.org/10.1023/B:JOFL.0000016292.00622.25>
- Griesser, J., Hetényi, G., Moser, M., Demarne, F., Jannin, V., Bernkop-Schnürch, A., 2017. Hydrophobic ion pairing: Key to highly payloaded self-emulsifying peptide drug delivery systems. *Int. J. Pharm.* 520, 267–274.  
<https://doi.org/10.1016/J.IJPHARM.2017.02.019>

- Gungor, S., Okyar, A., Erturk-Toker, S., Baktir, G., Ozsoy, Y., 2010. Ondansetron-loaded biodegradable microspheres as a nasal sustained delivery system: In vitro/in vivo studies. *Pharm. Dev. Technol.* 15, 258–265.
- Haffejee, N., Du Plessis, J., Muller, D.G., Schultz, C., Kotze, A.F., Goosen, C., 2001. Intranasal toxicity of selected absorption enhancers. *Pharmazie* 56, 882–888.
- Hentz, N.G., Richardson, J.M., Sportsman, J.R., Daijo, J., Sittampalam, G.S., 1997. Synthesis and characterization of insulin-fluorescein derivatives for bioanalytical applications. *Anal. Chem.* 69, 4994–5000.
- Hillery, A.M., Lloyd, A.W., Swarbrick, J., 2002. *Drug delivery and targeting: for pharmacists and pharmaceutical scientists.* CRC Press.
- Hintzen, F., Perera, G., Hauptstein, S., Müller, C., Laffleur, F., Bernkop-Schnürch, A., 2014. In vivo evaluation of an oral self-microemulsifying drug delivery system (SMEDDS) for leuprorelin. *Int. J. Pharm.* 472, 20–26.  
<https://doi.org/10.1016/j.ijpharm.2014.05.047>
- Huang, C.H., Kimura, R., Bawarshi-Nassar, R., Hussain, A., 1985. Mechanism of nasal absorption of drugs II: Absorption of L-tyrosine and the effect of structural modification on its absorption. *J. Pharm. Sci.* 74, 1298–1301.
- Illum, L., 2003. Nasal drug delivery—possibilities, problems and solutions. *J. Control. Release* 87, 187–198.
- Illum, L., 1991. The nasal delivery of peptides and proteins. *Trends Biotechnol.* 9, 284–289.
- Illum, L., Farraj, N.F., Critchley, H., Johansen, B.R., Davis, S.S., L. Illum 1, N.F. Farraj

- 1, H. Critchley 1, B.R.J. 2 and S.S.D. 1, 1989. Enhanced nasal absorption of insulin in rats using lysophosphatidylcholine. *Int. J. Pharm.* 57, 49–54.
- J.M. Pezzuto H.R. Manasse, M.E.J., 2013. *Biotechnology and Pharmacy, Biotechnology and Pharmacy.*
- Jacob, D., Joan Taylor, M., Tomlins, P., Sahota, T.S., 2016. Synthesis and Identification of FITC-Insulin Conjugates Produced Using Human Insulin and Insulin Analogues for Biomedical Applications. *J. Fluoresc.* 26, 617–629.  
<https://doi.org/10.1007/s10895-015-1748-1>
- Jintapattanakit, A., Junyaprasert, V.B., Mao, S., Sitterberg, J., Bakowsky, U., Kissel, T., 2007. Peroral delivery of insulin using chitosan derivatives: a comparative study of polyelectrolyte nanocomplexes and nanoparticles. *Int. J. Pharm.* 342, 240–249.
- Jitendra, P.K., Bansal, S., Banik, A., 2011. Noninvasive routes of proteins and peptides drug delivery. *Indian J. Pharm. Sci.* 73, 367.
- Jobbágy, A., Jobbágy, G.M., 1973. Examination of FITC preparations. II. Measurements of isothiocyanate content of fluorescein isothiocyanate preparations. *J. Immunol. Methods* 2, 169–181. [https://doi.org/10.1016/0022-1759\(73\)90014-8](https://doi.org/10.1016/0022-1759(73)90014-8)
- Kalluri, H., Banga, A.K., 2011. Transdermal delivery of proteins. *Aaps Pharmscitech* 12, 431–441.
- Karamanidou, T., Karidi, K., Bourganis, V., Kontonikola, K., Kammona, O., Kiparissides, C., 2015. Effective incorporation of insulin in mucus permeating self-nanoemulsifying drug delivery systems. *Eur. J. Pharm. Biopharm.* 97, 223–229.  
<https://doi.org/10.1016/j.ejpb.2015.04.013>

- Kaushal, G., Trombetta, L., Ochs, R.S., Shao, J., 2006. Delivery of TEM  $\beta$ -lactamase by gene-transformed *Lactococcus lactis* subsp. *lactis* through cervical cell monolayer. *Int. J. Pharm.* 313, 29–35. <https://doi.org/10.1016/J.IJPHARM.2006.01.013>
- Khan, J., Alexander, A., Ajazuddin, Saraf, S., Saraf, S., 2013. Recent advances and future prospects of phyto-phospholipid complexation technique for improving pharmacokinetic profile of plant actives. *J. Control. Release* 168, 50–60. <https://doi.org/10.1016/J.JCONREL.2013.02.025>
- Khatri, P., Shao, J., 2017a. Separation of external aqueous phase from o/w nanoemulsions. *Eur. J. Pharm. Sci.* 96, 171–175. <https://doi.org/10.1016/J.EJPS.2016.09.021>
- Khatri, P., Shao, J., 2017b. Transport of lipid nano-droplets through MDCK epithelial cell monolayer. *Colloids Surfaces B Biointerfaces* 153, 237–243. <https://doi.org/10.1016/J.COLSURFB.2017.02.024>
- Kissel, T., Werner, U., 1998. Nasal delivery of peptides: an in vitro cell culture model for the investigation of transport and metabolism in human nasal epithelium. *J. Control. Release* 53, 195–203.
- Klingler, C., Müller, B.W., Steckel, H., 2009. Insulin-micro-and nanoparticles for pulmonary delivery. *Int. J. Pharm.* 377, 173–179.
- Ko, K.-T., Needham, T.E., Zia, H., 1998. Emulsion formulations of testosterone for nasal administration. *J. Microencapsul.* 15, 197–205. <https://doi.org/10.3109/02652049809006849>
- Koga, K., Takarada, N., Takada, K., 2010. Nano-sized water-in-oil-in-water emulsion

enhances intestinal absorption of calcein, a high solubility and low permeability compound. *Eur. J. Pharm. Biopharm.* 74, 223–232.

Kumar, M., Pathak, K., Misra, A., 2009. Formulation and characterization of nanoemulsion-based drug delivery system of risperidone. *Drug Dev. Ind. Pharm.* 35, 387–395.

Lansley, A.B., 1993. Mucociliary clearance and drug delivery via the respiratory tract. *Adv. Drug Deliv. Rev.* 11, 299–327.

Lee, V.H., Yamamoto, A., Kompella, U.B., 1991. Mucosal penetration enhancers for facilitation of peptide and protein drug absorption. *Crit. Rev. Ther. Drug Carrier Syst.* 8, 91–192.

Li, P., Nielsen, H.M., Müllertz, A., 2016. Impact of Lipid-Based Drug Delivery Systems on the Transport and Uptake of Insulin Across Caco-2 Cell Monolayers. *J. Pharm. Sci.* <https://doi.org/10.1016/j.xphs.2016.01.006>

Li, Y., Lin, J., Liu, G., Li, Y., Song, L., Fan, Z., Zhu, X., Su, G., Hou, Z., 2016. Self-assembly of multifunctional integrated nanoparticles loaded with a methotrexate–phospholipid complex: combining simplicity and efficacy in both targeting and anticancer effects. *RSC Adv.* 6, 86717–86727. <https://doi.org/10.1039/C6RA17260A>

Lin, H., Li, H., Cho, H., Bian, S., Roh, H., Lee, M., Kim, J.S., Chung, S., Shim, C., Kim, D., 2007. Air-liquid interface (ALI) culture of human bronchial epithelial cell monolayers as an in vitro model for airway drug transport studies. *J. Pharm. Sci.* 96, 341–350.

- Lin, H., Yoo, J.-W., Roh, H.-J., Lee, M.-K., Chung, S.-J., Shim, C.-K., Kim, D.-D., 2005. Transport of anti-allergic drugs across the passage cultured human nasal epithelial cell monolayer. *Eur. J. Pharm. Sci.* 26, 203–210.
- Lindmark, T., Kimura, Y., Artursson, P., 1998. Absorption Enhancement through Intracellular Regulation of Tight Junction Permeability by Medium Chain Fatty Acids in Caco-2 Cells. *J. Pharmacol. Exp. Ther.* 284.
- Liu, H., Lu, H., Liao, L., Zhang, X., Gong, T., Zhang, Z., 2015. Lipid nanoparticles loaded with 7-ethyl-10-hydroxycamptothecin-phospholipid complex: *in vitro* and *in vivo* studies. *Drug Deliv.* 22, 701–709.  
<https://doi.org/10.3109/10717544.2014.895069>
- Ma, Z., Lim, L.Y., 2003. Uptake of Chitosan and Associated Insulin in Caco-2 Cell Monolayers: A Comparison between Chitosan Molecules and Chitosan Nanoparticles. *Pharm. Res.* 20, 1812–1819.  
<https://doi.org/10.1023/B:PHAM.00000003379.76417.3e>
- Martin, E., Schipper, N.G.M., Verhoef, J.C., Merkus, F.W.H.M., 1998. Nasal mucociliary clearance as a factor in nasal drug delivery. *Adv. Drug Deliv. Rev.* 29, 13–38.
- Martin, E., Verhoef, J.C., Romeijn, S.G., Merkus, F.W.H.M., 1995. Effects of Absorption Enhancers on Rat Nasal Epithelium *in Vivo*: Release of Marker Compounds in the Nasal Cavity. *Pharm. Res.* 12, 1151–1157.  
<https://doi.org/10.1023/A:1016207809199>
- Mathias, N.R., Timoszyk, J., Stetsko, P.I., Megill, J.R., Smith, R.L., Wall, D.A., 2002.

- Permeability characteristics of calu-3 human bronchial epithelial cells: in vitro-in vivo correlation to predict lung absorption in rats. *J. Drug Target.* 10, 31–40.
- Matsuyama, T., Morita, T., Horikiri, Y., Yamahara, H., Yoshino, H., 2006. Enhancement of nasal absorption of large molecular weight compounds by combination of mucolytic agent and nonionic surfactant. *J. Control. Release* 110, 347–352.
- McNay, E.C., Teske, J.A., Kotz, C.M., Dunn-Meynell, A., Levin, B.E., McCrimmon, R.J., Sherwin, R.S., 2013. Long-term, intermittent, insulin-induced hypoglycemia produces marked obesity without hyperphagia or insulin resistance: A model for weight gain with intensive insulin therapy McNay EC, Teske JA, Kotz CM, Dunn-Meynell A, Levin BE, McCrimmon RJ, Sherwin RS. Long-term, intermittent, insulin-induced hypoglycemia produces marked obesity without hyperphagia or insulin resistance: A model for weight gain with intensive insulin therapy. *Am J Physiol Endocrinol Metab* 304, 131–138.  
<https://doi.org/10.1152/ajpendo.00262.2012>
- Mitra, R., Pezron, I., Chu, W.A., Mitra, A.K., 2000. Lipid emulsions as vehicles for enhanced nasal delivery of insulin. *Int. J. Pharm.* 205, 127–134.
- Morimoto, K., Miyazaki, M., Kakemi, M., 1995. Effects of proteolytic enzyme inhibitors on nasal absorption of salmon calcitonin in rats. *Int. J. Pharm.* 113, 1–8.
- Moses, A.C., Gordon, G.S., Carey, M.C., Flier, J.S., 1983. Insulin administered intranasally as an insulin-bile salt aerosol. Effectiveness and reproducibility in normal and diabetic subjects. *Diabetes* 32, 1040–1047.
- Muheem, A., Shakeel, F., Jahangir, M.A., Anwar, M., Mallick, N., Jain, G.K., Warsi,

- M.H., Ahmad, F.J., 2014. A review on the strategies for oral delivery of proteins and peptides and their clinical perspectives. *Saudi Pharm. J.*
- Nash, R.A., Swarbrick, J., Boylan, J.C., 2002. *Encyclopedia of pharmaceutical technology.*
- Ozsoy, Y., Gungor, S., Cevher, E., 2009. Nasal delivery of high molecular weight drugs. *Molecules* 14, 3754–3779.
- Ozsoy, Y., Tuncel, T., Can, A., Akev, N., Birteksoz, S., Gerceker, A., 2000. In vivo studies on nasal preparations of ciprofloxacin hydrochloride. *Pharmazie* 55, 607–609.
- Piao, H.-M., Balakrishnan, P., Cho, H.-J., Kim, H., Kim, Y.-S., Chung, S.-J., Shim, C.-K., Kim, D.-D., 2010. Preparation and evaluation of fexofenadine microemulsions for intranasal delivery. *Int. J. Pharm.* 395, 309–316.  
<https://doi.org/10.1016/J.IJPHARM.2010.05.041>
- Pillai, O., Panchagnula, R., 2001. Insulin therapies—past, present and future. *Drug Discov. Today* 6, 1056–1061.
- Pires, A., Fortuna, A., Alves, G., Falcão, A., 2009. Intranasal drug delivery: how, why and what for?
- Prajapati, H.N., Dalrymple, D.M., Serajuddin, A.T.M., 2012. A comparative evaluation of mono-, di- and triglyceride of medium chain fatty acids by lipid/surfactant/water phase diagram, solubility determination and dispersion testing for application in pharmaceutical dosage form development. *Pharm. Res.* 29, 285–305.
- Rao, S.V.R., Agarwal, P., Shao, J., 2008a. Self-nanoemulsifying drug delivery systems

- (SNEDDS) for oral delivery of protein drugs: II. In vitro transport study. *Int. J. Pharm.* 362, 10–15. <https://doi.org/10.1016/J.IJPHARM.2008.05.016>
- Rao, S.V.R., Shao, J., 2008. Self-nanoemulsifying drug delivery systems (SNEDDS) for oral delivery of protein drugs: I. Formulation development. *Int. J. Pharm.* 362, 2–9.
- Rao, S.V.R., Yajurvedi, K., Shao, J., 2008b. Self-nanoemulsifying drug delivery system (SNEDDS) for oral delivery of protein drugs: III. In vivo oral absorption study. *Int. J. Pharm.* 362, 16–19. <https://doi.org/10.1016/J.IJPHARM.2008.05.015>
- Reddy, P.C., Chaitanya, K.S.C., Rao, Y.M., 2011. A review on bioadhesive buccal drug delivery systems: current status of formulation and evaluation methods. *DARU J. Pharm. Sci.* 19, 385.
- Riss, T.L., Moravec, R.A., Niles, A.L., Benink, H.A., Worzella, T.J., Minor, L., Storts, D., Reid, Y., 2004. Cell Viability Assays, in: Sittampalam, G.S., Coussens, N.P., Nelson, H., Arkin, M., Auld, D., Austin, C., Bejcek, B., Glicksman, M., Inglese, J., Iversen, P.W., Li, Z., McGee, J., McManus, O., Minor, L., Napper, A., Peltier, J.M., Riss, T., Trask OJ, J., Weidner, J. (Eds.), *Assay Guidance Manual*. Bethesda (MD). <https://doi.org/NBK144065> [bookaccession]
- Rogers, M. V., 1997. Light on high-throughput screening: fluorescence-based assay technologies. *Drug Discov. Today* 2, 156–160. [https://doi.org/10.1016/S1359-6446\(97\)01016-7](https://doi.org/10.1016/S1359-6446(97)01016-7)
- Sakai, M., Imai, T., Ohtake, H., Azuma, H., Otagiri, M., 1997. Effects of Absorption Enhancers on the Transport of Model Compounds in Caco-2 Cell Monolayers: Assessment by Confocal Laser Scanning Microscopy. *J. Pharm. Sci.* 86, 779–785.

<https://doi.org/10.1021/JS960529N>

Sarkar, M.A., 1992. Drug metabolism in the nasal mucosa. *Pharm. Res.* 9, 1–9.

Schmidt, M.C., Peter, H., Lang, S.R., Ditzinger, G., Merkle, H.P., 1998. In vitro cell models to study nasal mucosal permeability and metabolism. *Adv. Drug Deliv. Rev.* 29, 51–79.

Schroeder, N.E., Macguidwin, A.E., 2010. Behavioural quiescence reduces the penetration and toxicity of exogenous compounds in second-stage juveniles of *Heterodera glycines*. *Nematology* 12, 277–287.

<https://doi.org/10.1163/138855409X12506855979712>

Shao, Z., Li, Y., Krishnamoorthy, R., Chermak, T., Mitra, A.K., 1993. Differential Effects of Anionic, Cationic, Nonionic, and Physiologic Surfactants on the Dissociation,  $\alpha$ -Chymotryptic Degradation, and Enteral Absorption of Insulin Hexamers. *Pharm. Res.* 10, 243–251. <https://doi.org/10.1023/A:1018990928259>

Shinichiro, H., Takatsuka, Y., Hiroyuki, M., 1981. Mechanisms for the enhancement of the nasal absorption of insulin by surfactants. *Int. J. Pharm.* 9, 173–184.

[https://doi.org/10.1016/0378-5173\(81\)90010-7](https://doi.org/10.1016/0378-5173(81)90010-7)

Simon, M., Wittmar, M., Kissel, T., Linn, T., 2005. Insulin Containing Nanocomplexes Formed by Self-Assembly from Biodegradable Amine-Modified Poly(Vinyl Alcohol)-Graft-Poly(L-Lactide): Bioavailability and Nasal Tolerability in Rats.

*Pharm. Res.* 22, 1879–1886. <https://doi.org/10.1007/s11095-005-7676-z>

Sintov, A.C., Levy, H. V, Botner, S., 2010. Systemic delivery of insulin via the nasal route using a new microemulsion system: in vitro and in vivo studies. *J. Control.*

Release 148, 168–176.

Stafford, R.E., Dennis, E.A., 1987. Lysophospholipids as biosurfactants. *Colloids and Surfaces* 30, 47–64. [https://doi.org/10.1016/0166-6622\(87\)80203-2](https://doi.org/10.1016/0166-6622(87)80203-2)

Sudhakar, Y., Kuotsu, K., Bandyopadhyay, A.K., 2006. Buccal bioadhesive drug delivery—a promising option for orally less efficient drugs. *J. Control. Release* 114, 15–40.

Sun, S., Liang, N., Kawashima, Y., Xia, D., Cui, F., 2011. Hydrophobic ion pairing of an insulin-sodium deoxycholate complex for oral delivery of insulin. *Int. J. Nanomedicine* 6, 3049–3056. <https://doi.org/10.2147/IJN.S26450> [doi]

Trehan, A., Ali, A., 1998. Recent approaches in insulin delivery. *Drug Dev. Ind. Pharm.* 24, 589–597.

Ueno, T., Nagano, T., 2011. Fluorescent probes for sensing and imaging. *Nat. Methods* 8, 642–645. <https://doi.org/10.1038/nmeth.1663>

Ugwoke, M.I., Verbeke, N., Kinget, R., 2001. The biopharmaceutical aspects of nasal mucoadhesive drug delivery. *J. Pharm. Pharmacol.* 53, 3–22.

Winters, M.A., Knutson, B.L., Debenedetti, P.G., Sparks, H.G., Przybycien, T.M., Stevenson, C.L., Prestrelski, S.J., 1996. Precipitation of Proteins in Supercritical Carbon Dioxide. *J. Pharm. Sci.* 85, 586–594. <https://doi.org/10.1021/js950482q>

Xie, J., Li, Y., Song, L., Pan, Z., Ye, S., Hou, Z., Jiajiang Xie, Yanxiu Li, Liang Song, Zhou Pan, S.Y.& Z.H., 2017. Design of a novel curcumin-soybean phosphatidylcholine complex-based targeted drug delivery systems. *Drug Deliv.* 24, 707–719. <https://doi.org/10.1080/10717544.2017.1303855>

- Yoshida, T., Nishioka, H., Nakamura, Y., Kondo, M., 1985. Reduced noradrenaline turnover in streptozotocin-induced diabetic rats. *Diabetologia* 28, 692–696.  
<https://doi.org/10.1007/BF00291978>
- Yuba, E., Kono, K., 2014. Nasal Delivery of Biopharmaceuticals, in: *Mucosal Delivery of Biopharmaceuticals*. Springer, pp. 197–220.
- Zhang, Q., Zhang, L., Zhu, F., He, N., Chen, Q., Qin, Y., Zhang, Z., Zhang, Q., Wang, S., He, Q., 2012. The In Vitro and In Vivo Study on Self-Nanoemulsifying Drug Delivery System (SNEDDS) Based on Insulin-Phospholipid Complex ultrasound imaging View project A Young Female with Patent foramen ovale and Cryptogenic Stroke View project The In Vitro and In Vivo Study on Self-Nanoemulsifying Drug Delivery System (SNEDDS) Based on Insulin-Phospholipid Complex. *Artic. J. Biomed. Nanotechnol.* 8, 90–97. <https://doi.org/10.1166/jbn.2012.1371>
- Zhou, X.H., Po, A.L.W., 1990. Comparison of enzymic activities of tissues lining portals of drug absorption, using the rat as a model. *Int. J. Pharm.* 62, 259–267.

## Vita

**Name:**

*Darshana Shah*

**Baccalaureate Degree:**

*Bachelor of Science*

*Nitte Gulabi Shetty*

*Memorial Institute of*

*Pharmaceutical Sciences*

*Mangalore, India*

*Major: Pharmacy*

**Date Graduated:**

*December, 2006*

**Master's Degree:**

*Master of Science*

*St. John's University*

*Jamaica, New York, USA*

*Major: Pharmaceutical*

*Sciences*

**Date Graduated:**

*June, 2009*